

AD-760 173

LIQUID CRYSTAL SYSTEMS FOR ELECTRO-
OPTICAL STORAGE EFFECTS

Joseph A. Castellano, et al

RCA Laboratories

Prepared for:

Air Force Materials Laboratory

December 1971

DISTRIBUTED BY:

NTIS

National Technical Information Service
U. S. DEPARTMENT OF COMMERCE
5285 Port Royal Road, Springfield Va. 22151

AFML-TR-73-51

(1)

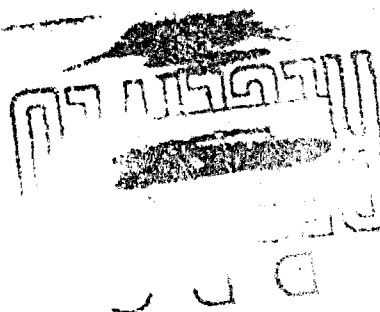
AD 760173

LIQUID CRYSTAL SYSTEMS FOR ELECTRO-OPTICAL STORAGE EFFECTS

BY

J. A. CASTELLANO, ET AL.

FINAL REPORT

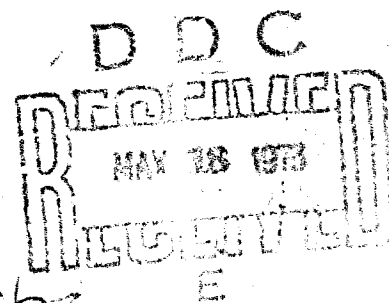


DECEMBER 1971

Approved for public release; distribution unlimited.

AIR FORCE MATERIALS LABORATORY
WRIGHT-PATTERSON AIR FORCE BASE, OHIO 45433

Best Available Copy



ACQUISITION FOR	
NTIS	WITH DATA <input checked="" type="checkbox"/>
U.S.	DATA <input type="checkbox"/>
CLASSIFIED	<input type="checkbox"/>
DISPOSITION	
BY	
DISPOSITION AVAILABILITY CODES	
DISC.	AVAIL. 2, 3, 4, 5, 6, 7, 8, 9, 10
A	

NOTICES

When Government drawings, specifications, or other data are used for any purpose other than in connection with a definitely related Government procurement operation, the United States Government thereby incurs no responsibility nor any obligation whatsoever; and the fact that the Government may have formulated, furnished, or in any way supplied the said drawings, specifications, or other data, is not to be regarded by implication or otherwise as in any manner licensing the holder or any other person or corporation, or conveying any rights or permission to manufacture, use, or sell any patented invention that may in any way be related thereto.

Qualified users may obtain copies of this report from DDC.

Copies of this report should not be returned unless return is required by security considerations, contractual obligations, or notice on a specific document.

AFML-TR-73-S1

LIQUID CRYSTAL SYSTEMS FOR ELECTRO-OPTICAL STORAGE EFFECTS

BY
J. A. CASTELLANO, ET AL.

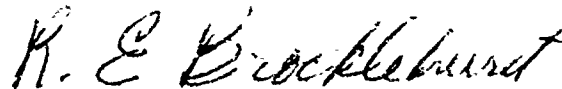
Approved for public release; distribution unlimited.

FOREWORD

This Final Report was prepared by RCA Laboratories, Princeton, New Jersey, under AF Contract No. F33615-70-C-1590, Project No. 7360. The work was administered under the direction of the Air Force Materials Laboratory. Dr. M. Berwick is the Air Force Project Engineer.

The report covers research conducted from June 15, 1970 through September 30, 1971, in the Communications Research Laboratory, K. H. Powers, Director. The Project Supervisor was D. A. Ross and the Project Scientist was J. A. Castellano. E. F. Pasierb, A. Sassman, C. S. Oh, D. Meyerhofer, M. T. McCaffrey and R. N. Friel contributed to the research and writing of this report.

The authors submitted this report on October 29, 1971. Submission of this report does not constitute Air Force approval of the report's findings or conclusions. It is submitted only for the exchange and stimulation of ideas.



ROBERT E. BROCKLEHURST
ASSISTANT CHIEF
ELECTROMAGNETIC MATERIALS DIVISION

ABSTRACT

Research on materials and electro-optic response measurements of certain cholesteric-nematic mixtures was performed in an effort to develop an optical storage display. Mixtures of selected compounds from the series, p-alkoxybenzylidene-p'-aminophenyl acrylates, were prepared and one ternary mixture (NH-1) which exhibited nematic behavior from 25 to 105°C was found. A group of optically active benzylidene aniline derivatives having alkoxy and acyloxy groups with asymmetric carbon atoms was prepared, and the compounds were found to exhibit cholesteric mesomorphism. Mixtures of these nonsteroidal cholesterics in the nematic compounds described above, however, were inferior to those prepared with the steroidal cholesterics. For example, cells made with a 7.5% cholesteryl oleate -- NH-1 mixture, which had a cholesteric range of 25 to 96°C, exhibited "writing" speeds of 5 to 10 msec and erasure speeds of 0.5 to 1.0 sec at room temperature with an ac drive signal of approximately 100 V (rms). This material was found to have a dielectric constant of 4.9 for the focal-conic texture and 5.8 for the planar texture. Light-scattering measurements led to a value of 1.6 μ m for the helical pitch. The mechanism of this effect involves changes from the stable (clear) planar texture of the cholesteric mesophase to the quasi-stable (scattering) focal-conic texture. A simulated, airborne ground location marker was constructed with a cell containing this material. In actual operation this device would provide the pilot or navigator of an aircraft with a map presentation of his past and present position as determined by two ground navigation stations.

DOCUMENT CONTROL DATA - R & D

(Security classification of title, body of abstract and indexing annotation must be entered when the overall report is classified)

1. ORIGINATING ACTIVITY (Corporate author) RCA Laboratories Princeton, New Jersey 08540		2a. REPORT SECURITY CLASSIFICATION Unclassified	
		2b. GROUP N/A	
3. REPORT TITLE LIQUID CRYSTAL SYSTEMS FOR ELECTRO-OPTICAL STORAGE EFFECTS			
4. DESCRIPTIVE NOTES (Type of report and inclusive dates) Final Report June 15, 1970 to September 30, 1971			
5. AUTHOR(S) (First name, middle initial, last name) Joseph A. Castellano, Ronald N. Friel, Michael T. McCaffrey, Dietrich Meyerhofer, Chan S. Oh, Edward F. Pasierb, and Alan Sussman			
6. REPORT DATE December 1971		7a. TOTAL NO. OF PAGES 61	7b. NO. OF REFS 19
8a. CONTRACT OR GRANT NO. F33615-70-C-1590		8b. ORIGINATOR'S REPORT NUMBER(S) PRRL-71-CR-35 AFML-TR-73-S1	
b. PROJECT NO. 7360		8c. OTHER REPORT NO(S) (Any other numbers that may be assigned this report)	
c.			
d.			
10. DISTRIBUTION STATEMENT This document is government property and its use is restricted to the Air Force.		Approved for public release; distribution unlimited. to foreign the Air	
11. SUPPLEMENT		Air Force Materials Laboratory Wright-Patterson AFB, OH 45433	
12. ABSTRACT Research on materials and electro-optic response measurements of certain cholesteric-nematic mixtures was performed in an effort to develop an optical storage display. Mixtures of selected compounds from the series, p-alkoxybenzylidene-p'-aminophenyl acylates, were prepared and one ternary mixture (NH-1) which exhibited nematic behavior from 25 to 105°C was found. A group of optically active benzylidene aniline derivatives having alkoxy and acyloxy groups with asymmetric carbon atoms was prepared, and the compounds were found to exhibit cholesteric mesomorphism. Mixtures of these nonsteroidal cholesterics in the nematic compounds described above, however, were inferior to those prepared with the steroidal cholesterics. For example, cells made with a 7.5% cholesteryl oleate - NH-1 mixture, which had a cholesteric range of 25 to 96°C, exhibited "writing" speeds of 5 to 10 msec and erasure speeds of 0.5 to 1.0 sec at room temperature with an ac drive signal of approximately 100 V (rms). This material was found to have a dielectric constant of 4.9 for the focal-conic texture and 5.8 for the planar texture. Light-scattering measurements led to a value of 1.6 μm for the helical pitch. The mechanism of this effect involves changes from the stable (clear) planar texture of the cholesteric mesophase to the quasi-stable (scattering) focal-conic texture. A simulated, airborne ground location marker was constructed with a cell containing this material. In actual operation this device would provide the pilot or navigator of an aircraft with a map presentation of his past and present position as determined by two ground navigation stations.			

14	KEY WORDS	LINK A		LINK B		LINK C	
		ROLE	WT	ROLE	WT	ROLE	WT
	Cholesteric Dielectric anisotropy Electro-optic response Liquid crystal Nematic Optical storage Scattering texture						

TABLE OF CONTENTS

Section	Page
I. INTRODUCTION	1
II. MATERIALS	3
A. General	3
B. Nematic Compounds	3
C. Cholesteric Compounds	8
D. Experimental	15
1. p-Alkoxybenzylidene-p'-aminophenyl Acylates	15
2. p-(Active-alkoxy)-benzylidene-p'-aminophenyl Acylates	15
3. p-n-Alkoxybenzylidene-p'-aminophenyl n-Alkyl Carbonates	16
4. Determination of Transition Temperatures	16
III. ELECTRO-OPTICAL BEHAVIOR	17
A. Materials Evaluated	17
B. Cell Fabrication	20
C. Reflectivity	21
D. Contrast Ratio	22
E. Static Electro-Optic Characteristics	23
F. Dynamic Electro-Optic Characteristics	25
G. Storage Properties	27
H. Device Thickness	30
I. Temperature Effects	30
J. Capacitance Measurements	31
K. Light-Scattering Characteristics	31
L. Material Resistivity	33
IV. LIGHT-SCATTERING BEHAVIOR	34
A. Experimental	34
B. Discussion of Results	42
V. MECHANISMS AND FUNDAMENTALS	43
VI. STATE-OF-THE-ART DEVICES	45
VII. CONCLUSIONS AND RECOMMENDATIONS	49
REFERENCES	51

LIST OF ILLUSTRATIONS

Figure	Page
1. Phase transition temperatures for the system $\text{ROC}_6\text{H}_4\text{CHNC}_6\text{H}_4\text{O}_2\text{CCH}_3$: Δ — Δ (nematic \rightarrow liquid); \blacksquare — \blacksquare (crystal \rightarrow mesomorphic)	5
2. Phase transition temperatures for the system $\text{CH}_3\text{OC}_6\text{H}_4\text{CHNC}_6\text{H}_4\text{OCOR}'$: Δ — Δ (nematic \rightarrow isotropic); \blacksquare — \blacksquare (crystal \rightarrow nematic).	6
3. Ternary phase diagram of compounds <u>1</u> (A), <u>4</u> (B), and <u>8</u> (C).....	7
4. Phase diagram of binary mixture containing $\text{C}_2\text{H}_5\underset{\text{CH}_3}{\underset{ }{\text{CH}}}-(\overset{*}{\text{CH}_2})_4-\text{O}-\text{C}_6\text{H}_4-\text{CH}=\text{N}-\text{C}_6\text{H}_4-\text{OCOC}_2\text{H}_5\text{(A)}$ and NH-1 (B): \square — cholesteric \rightarrow isotropic; Δ — smectic \rightarrow cholesteric; \circ — crystal \rightarrow mesomorphic (calculated)	15
5. Experimental setup for electro-optical response measurements	18
6. Brightness vs. voltage for four different nematic host materials	20
7. Reflectivity as a function of cholesteric content	21
8. Threshold field as a function of cholesteryl oleate content	24
9. Static electro-optic response of reflective storage cells	24
10. Dynamic electro-optic response of typical reflective storage cell	25
12. Response time as a function of voltage for three different nematic host materials	27
12. Segmented storage cell (top view)	30
13. Contrast ratio as a function of incidence and reflection angles	32
14. DC resistivity as a function of cholesteric components	33
15. Experimental arrangement for measuring light scattering of liquid crystal cells	35
16. Scattering intensity vs. detector angle	36
17. Voltage dependence of scattered light intensity	37
18. Schematic designation of Bragg scattering angles in the focal-conic texture	38
19. Angular light scattering intensity as a function of cholesteryl oleate content	39
20. Angular light scattering intensity as a function of cell thickness	39

LIST OF ILLUSTRATIONS (Continued)

Figure	Page
21. Scattering properties of two cells in series compared with a single cell	40
22. Angular light intensity as a function of incidence angle	41
23. Variation of scattered light intensity with angle of incidence	42
24. Schematic representation of electrically induced texture changes..	43
25. Liquid crystal panel for ground position locator .	45
26. Top view of storage cell with patterned transparent conducting stripes	46
27. Cross-sectional view showing louvered light control film	46
28. Simulated airborne ground position locator	47
29. Schematic diagram of simulated ground position locator .	48

LIST OF TABLES

Table	Page
I. Nematic p-Alkoxybenzylidene-p'-aminophenyl Acetates	5
II. Nematic p-Alkoxybenzylidene-p'-aminophenyl Acylates	6
III. $RO-C_6H_4-CH=N-C_6H_4-O-CO_2-R'$	9
IV. Monotropic Cholesteric Schiff Bases	11
V. Mesomorphic Behavior of Optically Active Benzylidene Anilines	13
VI. Materials Evaluation	19
VII. Reflectivity and Contrast of Cholesteric-Nematic Mixtures	22
VIII. Electro-Optic Response Characteristics	26
IX. Storage Behavior of Cholesteric-Nematic Mixtures	28
X. Attenuation of Direct Beam in Storage Cells of Various Thicknesses in the Storage State	39

SECTION 1 INTRODUCTION

The field of liquid crystals has developed into one of the most rapidly expanding areas of physical-chemical research. The use of certain cholesteric liquid crystals for medical diagnosis coupled with the discovery of several rather interesting and potentially important electro-optic effects in nematic liquid crystals has accelerated the growth of this field. In this report we shall discuss the results of our studies of electro-optical storage effects in mixtures of these two classes of liquid crystalline materials. These effects are expected to be applicable to a variety of information storage and retrieval display systems.

Most electronically controlled displays consist of devices and systems which present recurring signals that have a low repetition rate. Generally, some method of storage is required in order to retain the image for detailed examination; both direct-view and electrical readout methods have been employed. The most extensively used storage devices are special-purpose cathode-ray tubes. One type, the cathodochronic storage tube, uses photochromic phosphors to retain the image when electron beam addressing is complete. Erasure of the image is then achieved with heat or light of a particular wavelength. These displays are based on the emission of light and as a result require rather high voltage and power for their operation. Electronic control of reflected or scattered light through the use of liquid crystals, however, requires much lower power since the control circuitry does not supply energy for light emission. Thus, liquid crystal displays readily lend themselves to solid state addressing schemes.

Another important advantage of liquid crystal displays over those based on light emission is a contrast ratio which is independent of the ambient light intensity. Therefore, while the display is not visible in total darkness, it will not "wash-out" under high-intensity lighting conditions such as direct sunlight.

The optical storage effect is observed when a cell containing a cholesteric-type liquid crystal is activated by an electric field. In its quiescent state with no field applied, the liquid crystal is essentially transparent. When a dc or low-frequency (< 100 Hz) field of the order of 3×10^4 V/cm is applied, the liquid becomes opaque and scatters light. This white, opaque appearance (storage mode) is maintained after the dc voltage is removed. The material is returned to the original clear state (erase mode) by application of a high-frequency signal (> 500 Hz). Upon removal of the ac signal, the sample remains in its clear state. No electrochemical effects are noted when the sample is subjected to alternate store-erase excitation.

Thus, it is possible to produce either storage or erasure by application of a single form of energy (an electric field) merely by changing the frequency of the addressing signal. With cathodochronic storage tubes, on the other hand, the form of energy required for storage differs from that required for erasure, thus necessitating more complex system design.

The simplicity of the liquid crystal storage concept is demonstrated in the simulated ground location display (GLD) panel which was designed and built during the course of our research. This GLD unit merely consists of a compact, matrix-addressed display panel (16 square inches), several small batteries, and an oscillator. It is intended to provide the pilot or navigator of an aircraft (or spacecraft entering the earth's atmosphere) with a map presentation of the past and present position of his craft in relation to two separate ground stations. This information would enable the pilot to make the necessary adjustments in his course.

The major objectives of the present investigation are:

1. The development of liquid crystal systems which exhibit controlled, optical storage and have as wide an operating temperature range as possible (including, of course, room temperature).
2. The optimization of the display-related parameters such as storage time, contrast, writing and erasure speed.
3. The establishment of a model for the mechanism of the effect through an understanding of the optical properties of the various textures of the cholesteric mesophase.
4. The development of techniques to study and improve the operational lifetimes of the materials.
5. The design of matrix-type displays which simulate the operation of airborne indicators that provide the pilot with pictorial information on his position in relation to the ground.

SECTION II MATERIALS

A. GENERAL

Liquid crystallinity (or mesomorphism) has been described [1] as a new state of matter intermediate between a crystalline solid and a normal isotropic liquid. The phenomenon is generally exhibited by long, rod-shaped organic molecules which contain dipolar and polarizable groups. The mesophase exists over a very specific temperature range. Below this range the material is a solid and at higher temperatures it becomes an isotropic liquid. Both of these transitions are sharp and reproducible.

Friedel [1] carried out extensive optical studies on a number of mesomorphic materials and, as a result, he discovered three main types of mesomorphic states which he designated as the smectic, nematic, and cholesteric mesophase. The smectic mesophase is a turbid, highly viscous state with certain properties similar to those found for soaps. The term smectic is, in fact, derived from the Greek, *smectos* or soap-like. The smectic structure is stratified with the molecules arranged in layers; their long axes are parallel to each other in the layers and approximately normal to the plane of the layers. The molecules can move in two directions in the plane and they can rotate about one axis. Within the layers, which are approximately 20 Å thick, the molecules can be arranged either in neat rows or randomly distributed. In addition the planes can slide, without hindrance, over similar neighboring layers.

The term nematic was derived from the Greek word meaning thread because it describes the threadlike nature of the material as seen under the microscope. This liquid is characterized by a turbid, mobile appearance. The long axes of the molecules in this structure maintain a parallel or nearly parallel arrangement to each other. They are mobile in three directions and can rotate about one axis. This can be compared with a long cylinder of round pencils: the pencils can roll and slide back and forth but remain parallel to one another in the direction of their long axes.

The cholesteric mesophase is found primarily in derivatives of cholesterol, especially the esters. The structure consists of parallel, monomolecular layers in which the direction of the long axes of molecules in a chosen layer is slightly displaced from the direction of the axes of molecules in an adjacent layer. The displacement of direction continues from one layer to another resulting in a helical structure. This helical molecular ordering gives rise to a circular dichroism for light propagating parallel to the helical axis [2]. Thus, one particular wavelength of light of one sense of circular polarization is transmitted without attenuation while light of the opposite sense is totally reflected. Changes in the color of light reflected from the material as a function of temperature are attributed to changes in the pitch of the helix.

The cholesteric phase is often regarded as a special case of the nematic phase since it forms a structure having twisted nematic layers. If a small amount of optically active substance (such as a cholesteryl ester) is added to the normally nematic compound, the mesophase is transformed into a cholesteric mesophase. The helical twist angle of such mixtures has been shown to be a function of the concentration of the optically active compound [3].

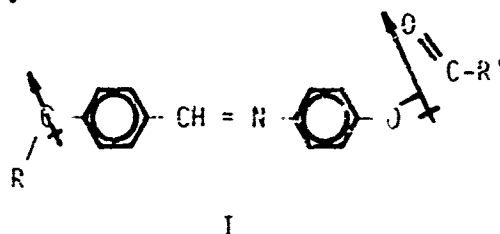
B. NEMATIC COMPOUNDS

A detailed discussion of the various textures which nematic materials adopt in thin layers is presented elsewhere [4] and, therefore, an extensive treatment of this subject will not be considered here. For the purposes of this discussion, however, it is appropriate to describe

briefly the so-called homeotropic and homogenous textures which are observed in thin layers between glass surfaces. The homeotropic texture is optically extinct between cross polarizers, while the homogenous texture is not. Both of these textures possess the optical properties of a positive uniaxial crystal. The texture observed depends upon the nature of the compound, the conditions used to obtain the mesophase, and the nature of the supporting surface.

In general, however, molecules which contain groups that permit the long axis to be strongly attracted to the glass surfaces will exhibit the homogenous texture while those molecules which are weakly attracted to the surface are most likely to form the homeotropic texture. Molecules which possess the former characteristic generally have a strong dipole moment along the long axis. In this case the dielectric constant (low frequency) parallel to the molecular axis is greater than the dielectric constant in the perpendicular direction, and the molecule is said to possess *positive dielectric anisotropy*. Conversely, molecules which have their dipole moment operating across the molecular axis generally exhibit the homeotropic texture and are said to possess *negative dielectric anisotropy*[4-7].

In order for the optical storage effect to be observed, the nematic molecules which are selected must have negative dielectric anisotropy. A series of compounds which meet these requirements is represented by structure I.

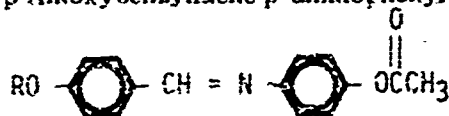


The parent compound in this series, p-anisylidene-p-aminophenylacetate ($R, R' = CH_3$), exhibits the storage effect when it is mixed with various cholesteryl esters[8]. This nematic compound, however, has a nematic range of 82 to 110°C. It was our intention, therefore, to prepare a number of compounds from series I which have lower crystal-nematic transition temperatures but still retain their nematic behavior at higher temperatures. This was accomplished by a systematic investigation of the effect of the length of alkoxy and acyloxy chains on the mesomorphic behavior of these compounds.

The first series of compounds with structure I was prepared by condensation of p-alkoxybenzaldehydes with p-aminophenylacetate. The water was removed azeotropically, and yields of 60 to 80% were generally obtained in refluxing benzene with benzenesulfonic acid catalyst. This series of compounds is listed in Table I while a phase transition plot is presented in Figure 1. This plot shows the typical behavior of a homologous series of Schiff bases, namely that the nematic-isotropic transition temperatures follow a smooth curve relationship when either the even or odd members are taken together. This is a well-known phenomenon[4] which has been found to occur with many other series. Note, however, that none of these compounds exhibits melting points below 79°C. Past experience has shown that further increases in the chain length result in the appearance of smectic behavior and in reduced nematic thermal stability.

When the alkyl chain in the ester portion of the molecule (R') was extended from C_2H_5 to $n-C_7H_{15}$ while the R group was maintained at CH_3 , lower melting compounds were obtained. These compounds were prepared by condensation of p-methoxybenzylidene-p-aminophenol with the appropriate anhydrides. The results of this study are presented in Table II while a phase transition plot is shown in Figure 2. (Several of these compounds have been reported by Kelker[9].) Although none of the compounds exhibited a crystal-nematic transition temperature at or near room temperature, several of them had melting points below 70°C. Again the nematic-isotropic transition temperature followed smooth curve relationships.

Table I
Nematic p-Alkoxybenzylidene-p'-aminophenyl Acetates^a



Compound	R	Smectic Range, °C	Nematic Range, °C
1	CH ₃	—	82-110 ^b
2	C ₂ H ₅	—	116-132
3	n-C ₃ H ₇	—	94-104
4	n-C ₄ H ₉	—	82-113
5	n-C ₅ H ₁₁	—	88-100
6	n-C ₆ H ₁₃	—	88-109
7	n-C ₇ H ₁₅	—	79-102.5
8	n-C ₈ H ₁₇	78-86	81-105.5
9	n-C ₉ H ₁₉	(81.5) ^c	86-100

(a) All compounds were purified by repeated recrystallization from hexane. A constant value of the nematic-isotropic transition constituted a pure sample [2].

(b) Hansen, Diss. Halle, 1907, reports a nematic range of 81.5 to 108°C.

(c) Monotropic smectic.

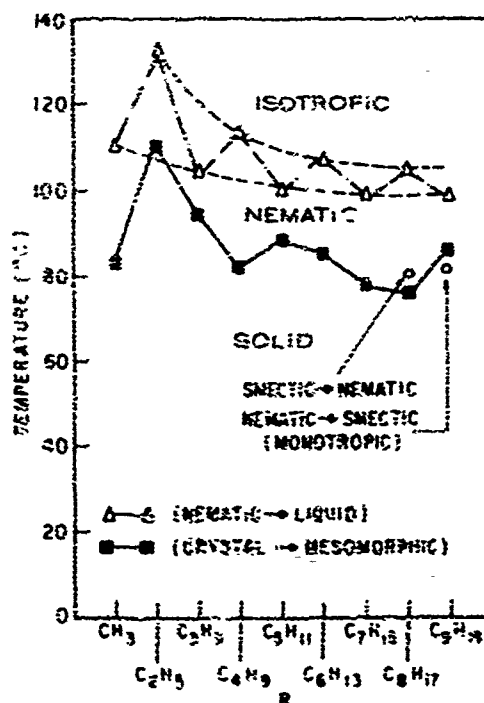
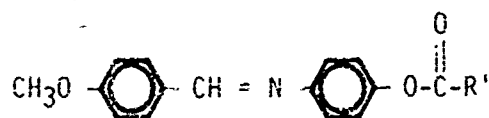


Figure 1. Phase transition temperatures for the system $\text{ROC}_6\text{H}_4\text{CHNC}_6\text{H}_4\text{O}_2\text{CCH}_3$: Δ — Δ (nematic → liquid); \blacksquare — \blacksquare (crystal → mesomorphic).

Table II
Nematic p-Alkoxybenzylidene-p'-aminophenyl Acylates



Compound	R'	Nematic Range, °C
10	C ₂ H ₅	70-109
11	C ₃ H ₇	53-112
12	C ₄ H ₉	55-100
13	C ₅ H ₁₁	81-100
14	C ₆ H ₁₃	64-96
15	C ₇ H ₁₅	67-99

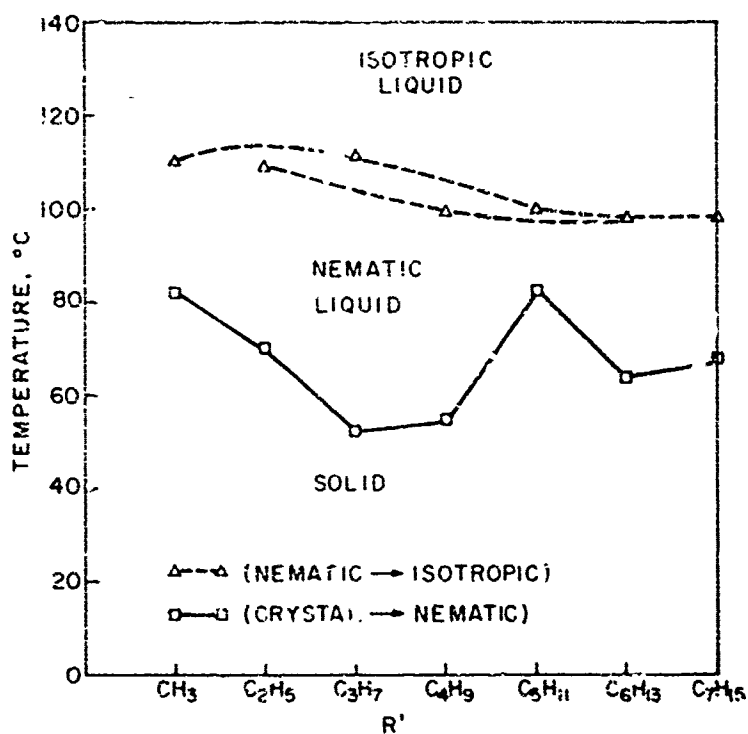


Figure 2. Phase transition temperatures for the system
CH₃OC₆H₄CHNC₆H₄OCOR': $\Delta \longrightarrow \Delta$ (nematic \rightarrow isotropic),
 $\square \longrightarrow \square$ (crystal \rightarrow nematic).

These results might lead one to conclude that further increases in the length of the chains in both the alkoxy and acyloxy groups would produce compounds with lower melting points, and wider nematic ranges. However, it has been found[4] that chain lengths of eight or more carbon atoms produce such weak terminal interactions that the critical balance of lateral-to-terminal attractive forces is upset, and the lateral interactions become important. An increase in the ratio of lateral-to-terminal cohesions always results[4] in the appearance of smectic behavior. Further increases in the chain length then result in increased smectic thermal stability and shorter nematic ranges. In order to produce materials from this class with lower melting points and wider nematic ranges, it was therefore necessary to use mixtures of these compounds.

Mixtures of non mesomorphic compounds with nematic compounds have been investigated previously. These systems are always characterized by a sharp decrease in both the nematic \rightarrow liquid and crystal \rightarrow nematic transition temperatures with increasing concentration of non-mesomorphic components[4].

Mixtures of two or more nematic compounds which possess subtle differences in molecular structure do not exhibit well-defined minima in their nematic \rightarrow liquid transition temperatures with molar composition although eutectic points for the crystal \rightarrow nematic transition temperatures are obtained. Thus, the nematic \rightarrow isotropic liquid transition temperatures form a smooth curve over the entire range of molar composition.

A series of binary and ternary mixtures from among several of the compounds of Tables I and II was therefore prepared. The compounds selected were those which had the lowest melting points and included 1, 4, 7, 8, 11, and 12.

The transition temperatures were measured and the data were used to construct a series of three-dimensional phase diagrams. A typical phase diagram of this type is that of Figure 3. Note that the nematic-isotropic transitions form a smooth, curved surface over all molar compositions.

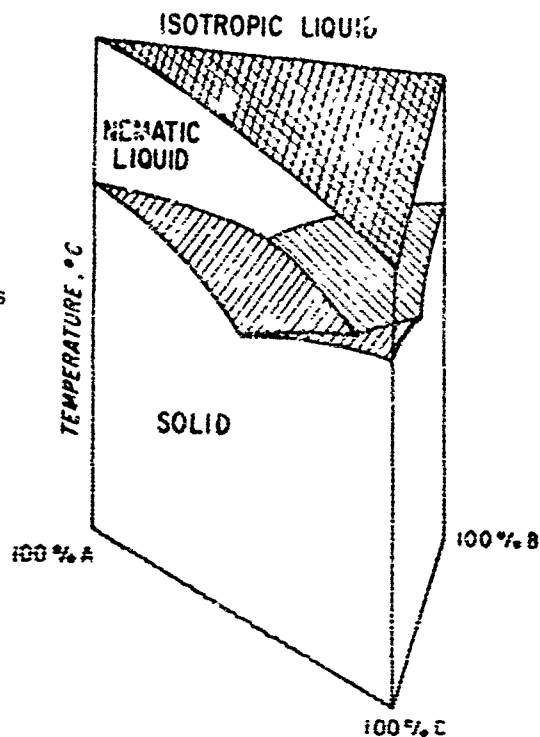
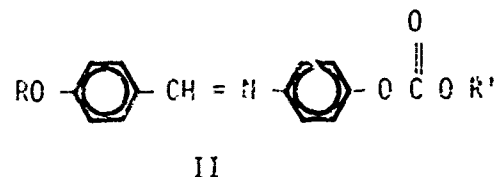


Figure 3. Ternary phase diagram of compounds 1(A), 4(B), and 8(C).

The mixture which had the lowest melting point and the widest nematic range was a ternary mixture consisting of equivalent quantities of compounds 1, 11, and 12. This mixture had a nematic range of 25 to 105°C and was subsequently used as the host material for our cholesteric compounds. This mixture is designated NH-1.

The second group of Schiff-base materials which we prepared under the Contract were p-alkoxybenzylidene-p'-aminophenyl alkyl carbonates (II)



In this series both R and R' were n-alkyl groups containing from 1 to 8 carbon atoms. The transition temperatures of the compounds are shown in Table III.

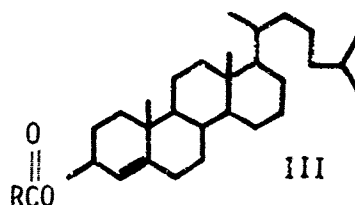
The lowest melting compounds in this series occurred when the R' group contained 5 or 6 carbon atoms. However, it should be noted that as the length of the alkyl chain in the alkoxy portion (R) increased beyond five carbon atoms in these compounds, smectic mesomorphism became apparent.

This is no doubt due to the increased separation of the dipolar end groups which tends to increase the ratio of lateral to terminal attractive forces.

A number of binary and ternary mixtures from among the compounds of Table III were prepared and their transition temperature measured. The ternary mixture containing 38% (by wt.) [≠16], 31.2% [≠17] and 30.8% [≠18] had a very broad nematic range (30 to 111°C) and was chosen as a second host material (designated NH-2) for our cholesteric material. The evaluation of both NH-1 and NH-2 is presented in a separate section below.

C. CHOLESTERIC COMPOUNDS

Compounds which exhibit the cholesteric mesophase are of two types. The first and most common type is the cholesteryl ester with the steroid structure III. The R group in this structure is generally a long alkyl chain: (C_nH_{2n+1}) containing from 1 to as many as 18



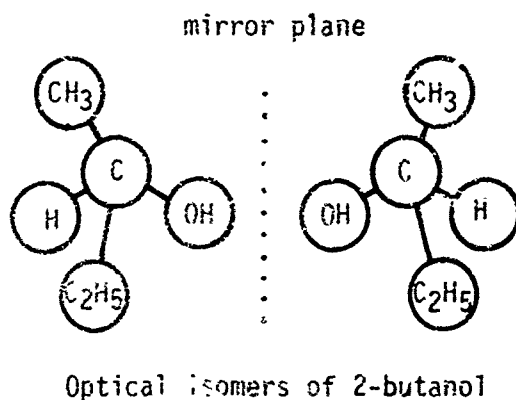
carbon atoms. These molecules are all optically active (vide infra) since they are derived from the natural product, cholesterol.

The second class of compounds which exhibit the "cholesteric" mesophase are not derivatives of cholesterol. These nonsteroidal cholesteric compounds have structures which are nearly identical to those of nematic compounds, with one important exception. That is, they possess an asymmetrically substituted carbon atom, which is a carbon atom bonded to four different atoms or groups.

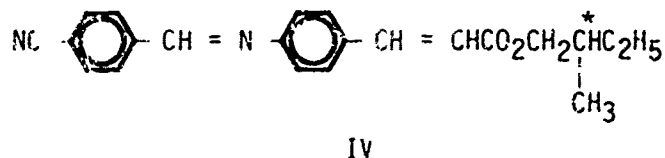
Table III
 $\text{RO-C}_6\text{H}_4\text{-CH=N-C}_6\text{H}_4\text{-O-CO}_2\text{-R'}$

Compound No.	F	R'	Smectic Range (°C)	Nematic Range (°C)
16	1	1	—	85-109
	2	1	—	86-132.5
	3	1	—	98-107
17	4	1	—	67-116
	5	1	—	91-106
18	6	1	62-64	65-108.5
	1	2	—	81-103.5
	2	2	—	94.5-129
	3	2	—	103.5-106
	4	2	—	89.5-114.2
	5	2	(46) ^a	82-104
	6	2	64.5-68	69-107.5
	7	2	(75)	76-102.5
	8	2	74-83	84-104.5
	1	3	—	78-86.5
	2	3	—	86-116
	3	3	—	84-95
	4	3	—	78-105.5
	5	3	—	65.5-96
	6	3	64-68	69-100
	7	3	67-73	74-95.5
	8	3	73-82	83-97
	1	4	—	66-84
	2	4	—	82-111.5
	3	4	—	69-93
	4	4	—	68.5-102.5
	5	4	—	71-95
	6	4	—	69-99
	7	4	65-69	70-94
	8	4	73-81	82-97
	1	5	—	75-81.5
	2	5	—	75-105
	3	5	—	58-108
	4	5	—	65-99
	5	5	—	66-93
	6	5	(58) ^a	63-96
	7	5	64-65	66-93
	8	5	73-79	80-95
	1	6	—	66-79
	2	6	—	71-102.5
	3	6	—	53-88
	4	6	—	56-97
	5	6	—	59.5-91
	6	6	(55) ^a	58-95.5
	7	6	62-63	64-92
	8	6	72-76	77-95
a) Monotropic				

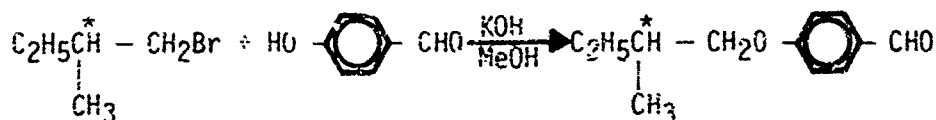
If a molecule has such an asymmetric center the molecule will be nonidentical with its mirror image* and will therefore be optically active. However, the chemical and physical properties of each form are identical. A simple example of an optically active compound is shown below:



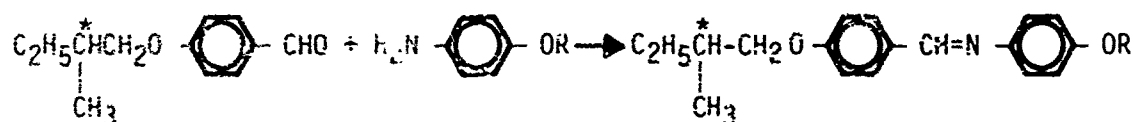
A nonsteroidal cholesteric compound which has been known for some time [4] is represented by structure IV.



During the contract period several series of optically active Schiff bases were prepared in an effort to produce new "cholesteric" liquid crystals. The first series of materials was prepared by the following synthetic route:



l-isomer



*Molecules which have two mirror image forms are said to possess chirality or handedness because they rotate the plane of polarized light in a left or right direction.

*Denotes asymmetric carbon atom.

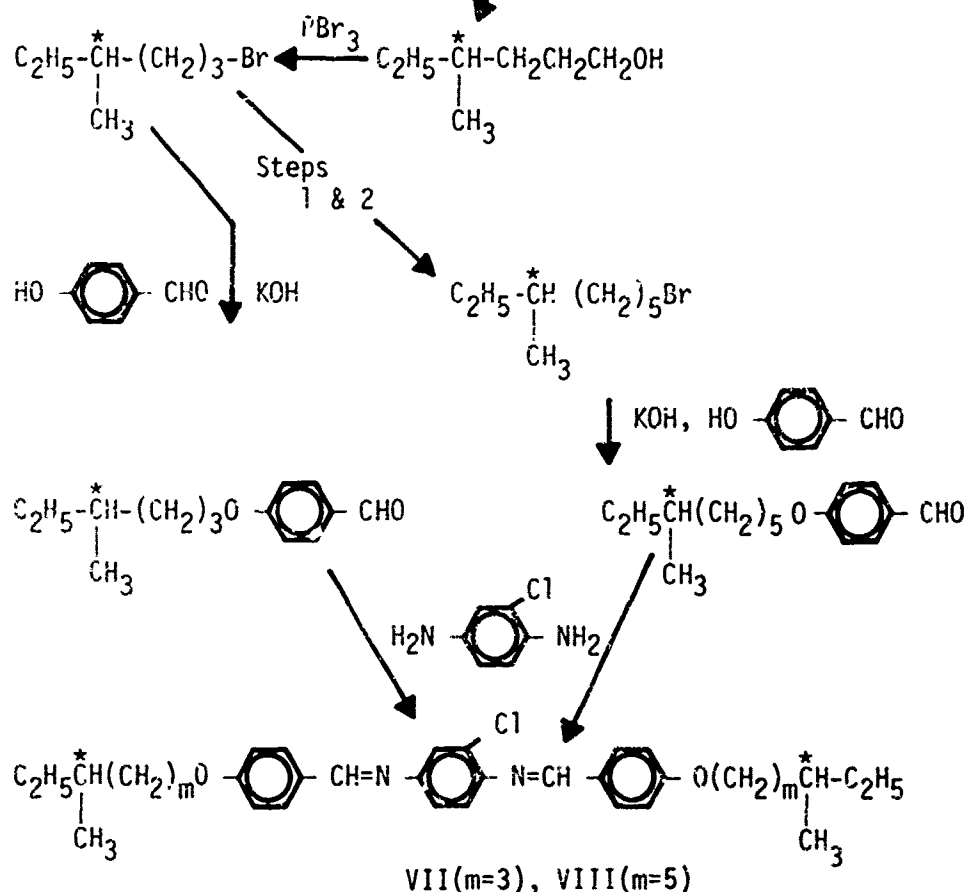
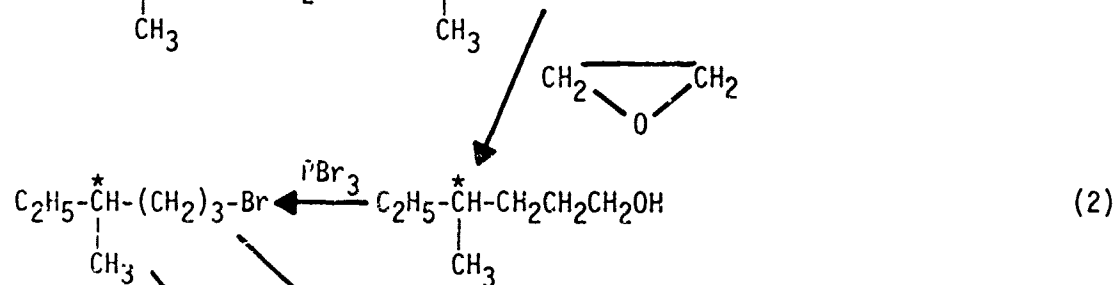
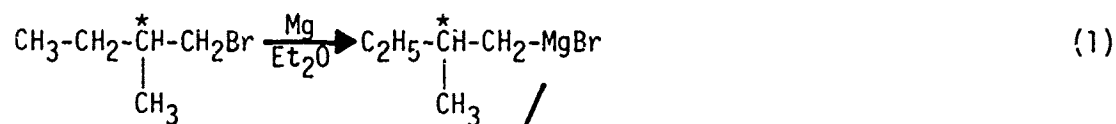
$$\text{C}_2\text{H}_5\overset{*}{\underset{\text{CH}_3}{\text{CH}}} - \text{CH}_2\text{O} - \text{C}_6\text{H}_4 - \text{CH} = \text{N} - \text{C}_6\text{H}_4 - \text{OC}(\text{R})=\text{O}$$

All of these materials were purified by repeated recrystallization from isopropanol to constant melting point.

$\text{CH}_3\text{CH}_2\overset{*}{\underset{\text{CH}_3}{\text{CH}}}-\text{CH}_2-\text{Br} \xrightarrow{\text{Mg}, \text{Et}_2\text{O}} \text{CH}_3\text{CH}_2\overset{*}{\underset{\text{CH}_3}{\text{CH}}}-\text{CH}_2-\text{MgBr} \xleftarrow{\text{CO}_2}$
 $\text{CH}_3\text{CH}_2\overset{*}{\underset{\text{CH}_3}{\text{CH}}}-\text{CH}_2-\text{CO}_2\text{H} \xrightarrow{\text{SOCl}_2} \text{CH}_3\text{CH}_2\overset{*}{\underset{\text{CH}_3}{\text{CH}}}-\text{CH}_2\text{COCl} +$
 $\longrightarrow \text{CH}_3\text{CH}_2-\overset{*}{\underset{\text{CH}_3}{\text{CH}}}-\text{CH}_2-\overset{\text{O}}{\parallel}\text{C}-\text{O}-\text{C}_6\text{H}_4-\text{NO}_2 \xrightarrow{\text{H}_2, \text{Pd(c)}} \longrightarrow \text{CHO}$
 $\text{CH}_3\text{CH}_2-\overset{*}{\underset{\text{CH}_3}{\text{CH}}}-\text{CH}_2-\overset{\text{O}}{\parallel}\text{C}-\text{O}-\text{C}_6\text{H}_4-\text{N}=\text{CH}-\text{C}_6\text{H}_4-\text{OCH}_3$
VI

- Monotropic mesomorphism is defined as that which is observed only upon cooling of the isotropic liquid.
- Enantiotropic mesomorphism occurs above the melting point of the compound and is observed both on heating from the mesomorphic state and cooling of the isotropic liquid.

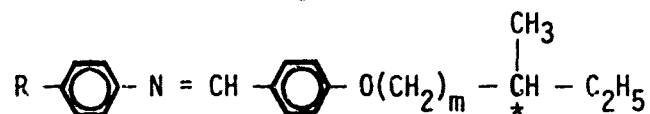
The next class of Schiff bases to be studied were the derivatives of 2-chlorophenylaniline which were prepared by the following route:



Both of these compounds exhibited a smectic and a cholesteric mesophase. However, the cholesteric mesophase appeared at higher temperatures.

	C-S	S-Ch	Ch-I
VII	43.5	50	146
VIII	29	94	146

The synthetic route shown above was extended to conventional two-ring Schiff bases and the resulting compounds exhibited the following behavior:



where $m = 3$, $R = \text{CH}_3\text{O} \rightarrow \text{C}_6\text{H}_{13}\text{O}$.

The melting points in this series were rather high (above 100°C) and enantiotropic mesomorphism was absent. The $\text{C}_2\text{H}_5\text{O}$ derivative had a monotropic cholesteric mesophase at 98° , while the higher homologs had only monotropic smectic phases.

$m = 3$, $R = \text{CH}_3, \text{C}_4\text{H}_9$.

These compounds were low melting, smectic materials.

$m = 3$, $R = \text{COC}_2\text{H}_5, \text{COC}_4\text{H}_9$.

These compounds showed a wide smectic range.

$m = 3$, $R = \text{OCO-CH}_3 \rightarrow \text{OCO-C}_7\text{H}_{15}$.

The transition temperatures for the compounds with $m = 4$ and 5 are shown in Table V. All of the compounds exhibited both smectic and cholesteric mesophases with the latter mesophase observable above 50°C . Most of the compounds showed two smectic mesophases. These phases were identified by differential scanning calorimetry and microscopic observation.

Table V
Mesomorphic Behavior of Optically Active Benzyldene Anilines

Compound No.	R	m	Crystal-S ₂	S ₂ -S ₁	S ₁ -Ch	Ch-l
19	CH ₃	4	48	—	56	72
20	C ₂ H ₅	4	41	—	61	82
21	n-C ₃ H ₇	4	49	—	64	83
22	n-C ₄ H ₉	4	37	—	74	79.5
23	n-C ₅ H ₁₁	4	46	74.5	77	84
24	n-C ₆ H ₁₃	4	72	73.5	79	82
25	n-C ₇ H ₁₅	4	57	72	82	85
26	CH ₃	5	69	69.5	71	83
27	C ₂ H ₅	5	54	81	82.5	92
28	n-C ₃ H ₇	5	37	85	87	94
29	n-C ₄ H ₉	5	—	86	89	90
30	n-C ₅ H ₁₁	5	52	85	92	93
31	n-C ₆ H ₁₃	5	57	88	95*	—
32	n-C ₇ H ₁₅	5	52	86.5	97*	—

*No cholesteric mesophase observed.

The increasing length of the alkyl chains in both the ether and ester portions of the molecule produces weaker terminal attractive forces relative to the lateral cohesive forces and, as a result, smectic thermal stability rises. Thus, compounds 31 and 32 have the highest smectic thermal stability and no cholesteric mesophase is present.

It is possible to drastically reduce smectic stability of these compounds by mixing them with various nematic compounds.

For example, a series of mixtures of 20 in NH-1 were prepared and these transition temperatures measured. A phase diagram illustrating these results is presented in Figure 4. Note that the smectic-nematic transition decreases sharply with decreasing concentrations of the optically active component, and at concentrations below ~30% the material exhibits only the cholesteric mesophase. All of the mixtures tended to supercool far below their "theoretical" crystal-mesomorphic transition temperature, and thus accurate melting point determinations could not be obtained for most of the mixtures (the presence of a glassy state was noted in these mixtures). The "theoretical" crystal-mesomorphic transitions shown in Figure 4 were calculated from the standard cryoscopic equation which is derived from the Clausius-Clapeyron equation. This derivation is based on a number of assumptions and would not be expected to hold except at low concentrations (ideal dilute solutions) of one component (solute) in the other (solvent). The equation is given by:

$$\frac{d \ln x}{dT} = \frac{L_f}{RT^2} \quad (\text{modified van't Hoff equation})$$

where x is the mole fraction of the "solvent," L_f is the molar heat of fusion (assuming that Raoult's law is applicable) and $R = 1.9869 \text{ cal}^\circ \text{ mole}$. When x is unity (pure "solvent") the melting point is T_0 and integration between T and T_0 (assuming L_f to remain constant) gives.

$$\ln x = \frac{-L_f}{R} \left(\frac{1}{T} - \frac{1}{T_0} \right)$$

or

$$T = \frac{T_0}{1 - \frac{RT_0}{L_f} \ln x}$$

where T is the calculated melting point of the mixture. Although this is a crude approximation, we have found [10] that it is possible to determine the composition of the eutectic mixture using this calculation. The experimental value of the melting points of any particular eutectic mixture, however, generally differs from that predicted by the modified van't Hoff equation. This is to be expected since these mixtures are not ideal, dilute solutions.

In any case, the significant result here is that smectic mesomorphism gives way exclusively to cholesteric mesomorphism at low concentrations of the optically active compound. Evaluation of these materials is presented in Section III.

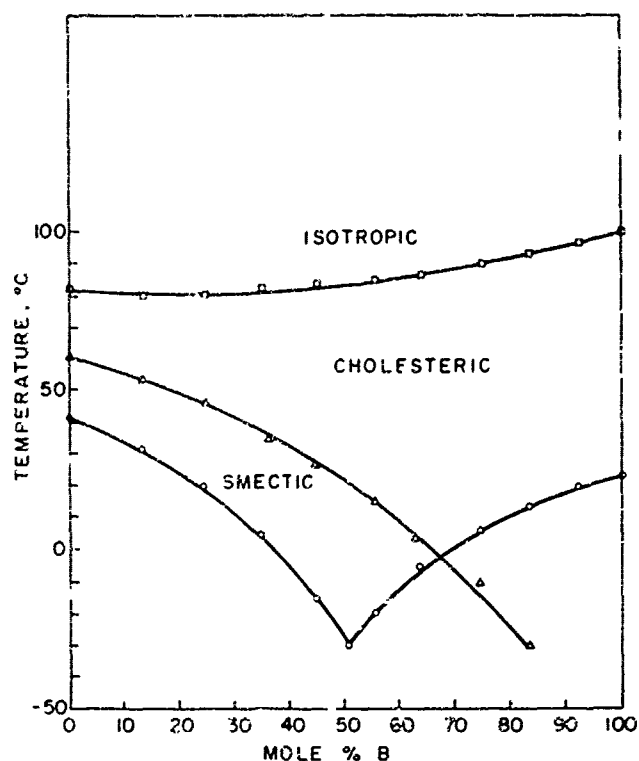
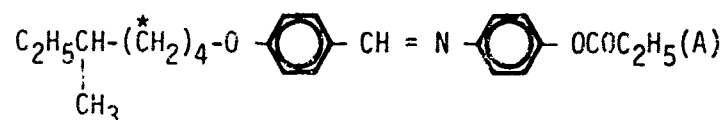


Figure 4. Phase diagram of binary mixture containing



and NH-1 (B): □ — cholesteric → isotropic; Δ — smectic → cholesteric; ○ — crystal → mesomorphic (calculated).

D. EXPERIMENTAL

1. p-Alkoxybenzylidene-p-aminophenyl Acylates

Previously described procedures[11,12] were used for these preparations. The components were recrystallized from isopropanol until the transition temperatures were constant and reversible.

2. p-(Active-alkoxy)-benzylidene-p-aminophenyl Acylates

Equimolar quantities of the corresponding aldehyde and amine were refluxed in ethanol for 30 minutes. Upon cooling, white crystals were obtained, and they were recrystallized several times from ethanol or isopropanol until sharp transition temperatures were obtained.

The p-active-alkoxybenzaldehydes were obtained from the corresponding active alkyl bromide and p-hydroxybenzaldehyde by refluxing in cyclohexanone with anhydrous potassium carbonate[13]. The optically active alcohols were synthesized from active amyl bromide via the Grignard reaction with paraformaldehyde and/or ethylene oxide[14]. Treatment[15] of the alcohols with PBr_3 yielded the optically active alkyl bromides.

3. p-n Alkoxybenzylidene-p'-aminophenyl n-Alkyl Carbonates

p-Aminophenyl n-alkyl carbonates were obtained by catalytic hydrogenation of the nitro derivative which was synthesized from p-nitrophenyl and the corresponding n-alkyl chloroformates. For example, the preparation of p-aminophenyl n-butyl carbonate was carried out in the following manner. Into an ether solution of 0.1 M. p-nitrophenol, 0.1 M. n-butylchloroformate (dissolved in ether) was added drop-wise at such a rate that the reaction mixture refluxed mildly. The reaction mixture was stirred for 8 hr and the resultant white solids were filtered off. The filtrate was washed with 200 ml of 0.1 N sodium hydroxide solution followed by several washings with saturated sodium chloride solution. The ether was evaporated and the resultant yellow oil was dissolved in chloroform and filtered through a short column of silica gel to eliminate the trace amount of phenol. After evaporation of chloroform, the product was vacuum-distilled to yield light-yellow p-nitrophenyl n-butyl carbonate (90% yield, gave a single spot in TLC examination).

0.1 M of this compound was then dissolved in 300 ml of anhydrous methanol containing 0.5 g of 10% palladium on charcoal. The mixture was shaken in a Parr hydrogenator until quantitative hydrogenation occurred (ca. 15 minutes). The methanol solution was filtered and evaporated under reduced pressure to about 50 ml. This operation was performed under a nitrogen atmosphere. The product which gave a single spot on TLC examination was transferred to a 100.0-ml volumetric flask, and a sufficient amount of isopropanol was added to the mark. Aliquots of 20.0 ml (0.02 M) were reacted with the corresponding aldehydes, and the products were purified by recrystallization as described above.

4. Determination of Transition Temperatures

Transition temperatures were determined with both a Thomas-Hoover melting point apparatus and a differential scanning calorimeter (DuPont Model 906 Thermal Analyzer). In the latter case, sample sizes were between 5 and 15 mg while the heating rate was 10° per minute. The transition temperatures were reproducible within 1°. The textures of the mesophases were examined with a Bausch and Lomb polarizing microscope equipped with a hot stage (magnifications were between 60 and 120X).

The smectic-cholesteric transitions of the mixture of 20 and NH-1 were observed in a Tenney Jr. refrigeration cabinet.

SECTION III ELECTRO-OPTICAL BEHAVIOR

In any type of display media there are a number of performance aspects that are extremely important but can usually be compromised for other system "trade-offs". For instance, in a field-controlled reflective optical storage device both the absolute reflectivity and contrast ratio might be suitably modified at the expense of response times and addressing conditions. Storage and life requirements, dictated primarily by specific applications, could possibly impose material restrictions that inherently limit device operating field "on" characteristics. The unique molecular architecture of the nematic-cholesteric liquid crystalline systems under study allowed a number of electro-optical properties to be investigated and modified, if necessary, to optimize device objectives.

Present experiments were based on the changes of such optical properties as scattering, reflection, birefringence, and, to some extent, color as affected by material composition, electric fields, operating temperature, and cell fabrication techniques. Most of the pertinent electro-optic characteristics of reflective storage cells were measured with the simple apparatus shown in the block diagram [Figure 5(a)]. The experimental setup illustrated in Figure 5(b) was used to measure the transmitted light-scattering properties.

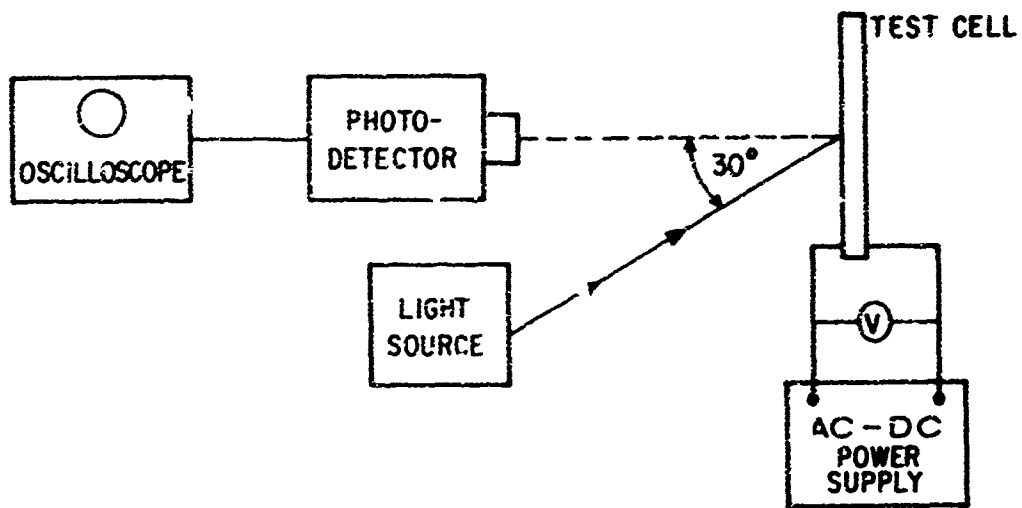
Reflectivity measurements were made by comparison with reflectance cards calibrated on a Munsell 17-step neutral value scale. This technique eliminated errors introduced by drift in amplifier gain and changes in incident light intensity. Storage and life properties were monitored for periods ranging from 3 weeks to 4 months. The accumulated data from these tests provided a qualitative comparison of materials behavior under room ambient conditions with no special efforts to improve storage or life performance. Such requirements should be realistically defined by specific display objectives.

Additional tests were undertaken to estimate operational lifetime expectancy and to determine the angular light-scattering distribution of typical storage mode devices. Measurements of capacitance, resistivity, and temperature effects were also made to further elucidate the mechanism of the storage-mode effect and to relate dynamic and static electro-optic properties to material composition. The following sections describe our materials and device evaluation program in terms of optimizing such display-related parameters as reflectivity, contrast, response speed, electric field requirements, and storage time.

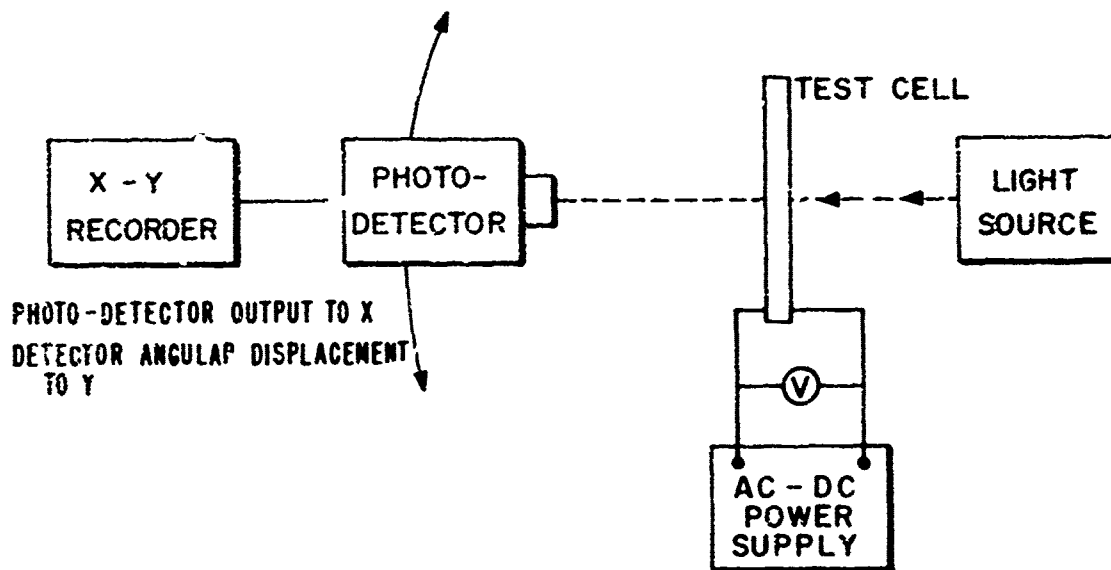
A. MATERIALS EVALUATED

During the initial phase of our materials evaluation program, measurements of electrical and optical characteristics were made more on a comparative than an absolute basis. In order to facilitate materials comparison in terms of display objectives, experimental tests were conducted with "standard" cells at room temperature, excited with electric fields limited to a narrow range of frequency and field strength. This technique allowed rapid elimination of those liquid crystalline compounds which did not appear to satisfy display-related parameters.

No extended effort was made to accurately relate physical and chemical properties with electro-optic performance during this investigation period. It was believed that such a cursory evaluation of material properties on a comparative basis was an expedient means of effectively selecting those materials and material combinations that would most likely satisfy device requirements.



(a) Reflective Measurements.



(b) Transmission Measurements.

Figure 5. Experimental setup for electro-optical response measurements.

The liquid crystal materials used in this study contained from 2% to 50% (by weight) of the selected cholesteric materials in the nematic mixtures described above (referred to as the nematic hosts in Section II). Initially, our materials evaluation program consisted primarily of determining electro-optic response behavior as affected by concentration of the cholesteric component. Specifically, mixtures made with 2, 5, 7.5, 10, 15, 20, and 50% cholesteryl oleate component and also 10, 20, and 50% cholesteryl chloride in the nematic host were prepared, and cells made with each of those mixtures were fabricated and measured.

The criterion by which the cholesteric-nematic systems under investigation were evaluated was their ability to modify incident light (reflection, contrast ratio) at moderate excitation voltages and to retain their scattering texture over a reasonable period of time with no maintaining power. Except for the materials containing less than 2% or greater than 20% cholesteric component, all of the mixtures satisfied these requirements to some degree. Electro optic behavior of materials containing less than 2% cholesteric component was similar to that of dynamic scattering while devices made with materials having greater than 20% cholesteric component exhibited cholesteric type characteristics. The electro-optic properties of cells fabricated with 5 to 10% cholesteryl oleate were found to compromise the characteristics of devices operating in the storage mode.

Having established the 5 to 10% range as an optimum concentration, another group of cholesteryl derivatives was evaluated in terms of display properties. Mixtures containing ~7.5% of the selected cholesteryl ester in the nematic host (NH-1) were prepared, and the electro-optic response of each mixture was measured and compared with a standard parallel plate cell fabricated with the 7.5% cholesteryl oleate formulation. Listed below are the materials that were evaluated.

Table VI
Materials Evaluation

Compound	Weight % in Nematic Host
1. Chol. Erucyl Carbonate	7.45
2. Chol. Oleyl Carbonate	7.69
3. Chol.-2(2-Butoxy Ethoxy)Ethyl Carbonate	7.17
4. Chol.-2-Methoxy-Ethoxy Carbonate	7.11
5. Chol. Geranyl Carbonate	7.45
6. Chol. Methane Sulfonate	7.50
7. Chol. Myristate	7.44
8. Chol. Nonanoate	7.52

Similarly, selected mixtures of the nonsteroidal cholesteric compounds described above (Section II) and both sitosteryl oleate and its hydrogenated derivative in NH-1 were evaluated. None of the mixtures exhibited electro-optic characteristics comparable with those of the cholesteryl oleate - nematic mixture. In general, response speeds were longer, excitation fields were higher, and storage life was considerably shorter.

To complete the materials investigation program, another nematic host, designated NH-2, was formulated and its electro-optic response compared with that of the NH-1 material. A plot of relative brightness vs. applied voltage for these two materials and two commercially available nematics is illustrated in Figure 6. Under this set of experimental conditions, NH-1 gave higher

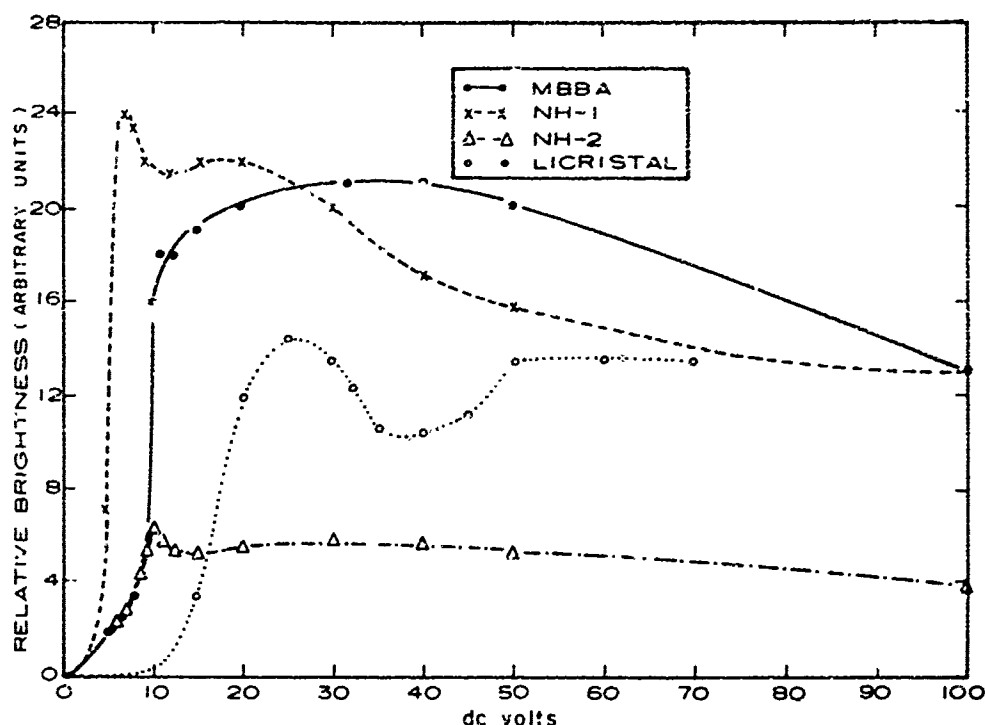


Figure 6. Brightness vs. voltage for four different nematic host materials.

contrast ratios at lower voltages than either the well-known MBBA (anisylidene-p-aminobutylbenzene) or LICRISTAL[®] (p-methoxy-p'-butylazoxy-benzene). On the other hand, NH-2 gave much lower contrast ratios than the other materials. This is believed to be due to the fact that this material spontaneously adopts the homogeneous (weakly scattering) texture between the electrodes. The maximum contrast ratio is always obtained when the unactivated material adopts the homeotropic (clear) texture.

The accumulated data of these experimental tests clearly show that the cholesteryl oleate NH-1 nematic mixture, particularly in the 5 to 10% composition range, is the optimum choice of material to allow superior device properties in terms of display related parameters. The mixture containing 7.5% cholesteryl oleate had a cholesteric range of 25 to 96°C.

B. CELL FABRICATION

Evaluation of each of the new materials was accomplished by measuring the phenomenological effects of a typical device structure. This structure is in the form of a parallel-plate capacitor consisting of two electrically conducting glass plates. The conducting film on at least one of these plates was transparent such as tin oxide coated or sputtered indium oxide. In the reflective mode of operation, the second glass plate was coated with a thin, evaporated layer of aluminum. The nematic-cholesteric mixture is sandwiched between the electrodes using teflon spacers of adequate thickness. Capillary action is sufficient to hold the liquid between the plates for a variety of orientations. Active area for all of the test units was 2.25 cm² although larger-area cells were often fabricated to simulate typical display conditions.

©E Merck & Co., Darmstadt, West Germany

For all of the comparative experimental tests, spacing between the conducting glass plates was 0.5 mil. Variations were made to determine the thickness dependence of such electro-optic properties as reflectivity, addressing requirements, storage capabilities and light-scattering characteristics. Improved dynamic response was observed with much thinner cells (0.25 mil or less) at the expense of long-time storage capabilities. A typical 4 in. x 4 in. display, however, often required thicker cells due to technological limitations in maintaining narrow spacings over a relatively large area and also to minimize the capacitive load on the electronic addressing circuitry.

Modification of the glass electrode surfaces by mechanical rubbing in order to improve electro-optic characteristics was attempted in the fabrication of a number of experimental devices. This technique should influence the molecular alignment of the cholesteric-nematic mixture at or near the liquid crystal/glass interface — especially in thin cells where surface-to-bulk effects should predominate — and was expected to affect the clarity of the storage device in the "clear" state after the excitation field was removed. No significant improvements in contrast ratio were observed in the tested units, and time limitations did not allow a continued research investigation of this fabrication technique.

C. REFLECTIVITY

The reflectivity of the cholesteryl oleate and cholesteryl chloride (in NH-1) combinations investigated during the reporting period is shown in Figure 7. For these measurements, a reflecting aluminum coating was evaporated to one of the glass plates, and the experimental setup was the same as shown in Figure 5(a). It is emphasized here that these data should be accepted as comparative behavior of the LC cells under specific test conditions. Exact values of reflection and contrast vary with incidence angle and parallelness of the illuminating source, the location and angular acceptance of the photodetector, and the light-scattering properties of the complete cell structure

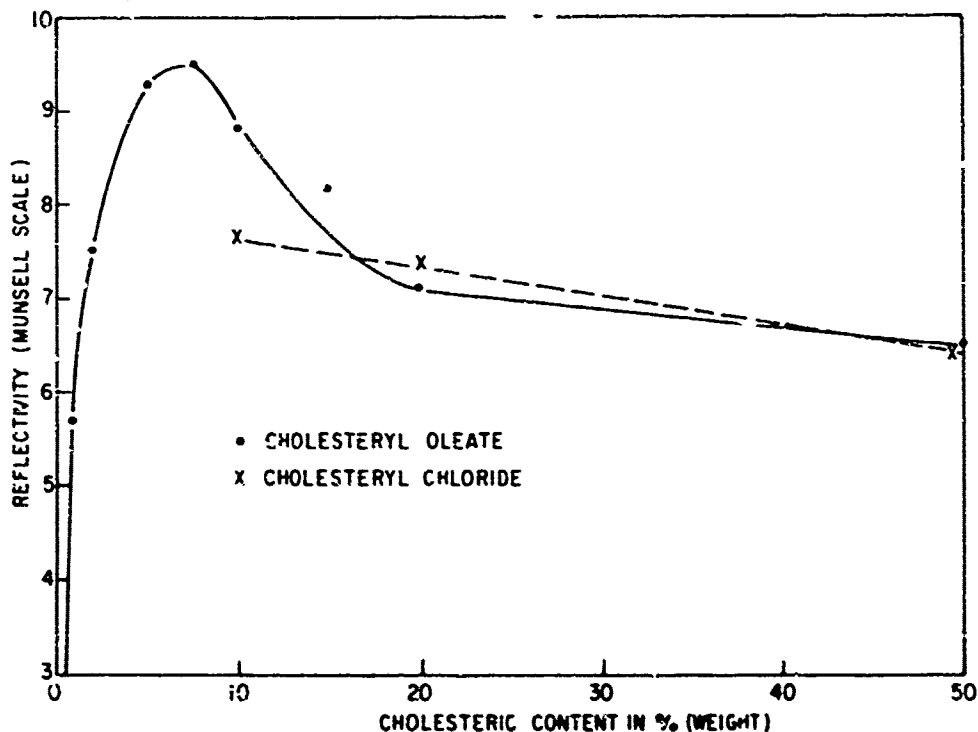


Figure 7. Reflectivity as a function of cholesteric content.

(reflecting or transparent back electrode). To simplify the interpretation of these measurements each cell was graded on a 17-step Munsell neutral value scale. That is, the reflection of each test unit was closely matched to a corresponding reflecting surface calibrated on a scale of 1.5 to 10.

The reflectivity value of each test cell was measured immediately after removal of the excitation field required to produce maximum light scattering. Units having between 5 and 10% cholesteryl oleate were generally found to be more reflective than those units made from other nematic-cholesteric systems. Table VII lists the reflectivity of some representative mixtures evaluated.

Table VII
Reflectivity and Contrast of Cholesteric-Nematic Mixtures

Cholesteryl Component	Weight % in Nematic Host	Reflectivity (Munsell Scale)	Contrast Ratio
1. Chol. Oleate	5.0	9.1	3.1:1
2. Chol. Chloride	5.0	8.2	1.5:1
3. Chol. Oleate	10	8.6	2.8:1
4. Chol. Chloride	10	7.7	1.4:1
5. Chol. Oleate	20	7.1	2:1
6. Chol. Chloride	20	7.3	1.3:1
7. Chol. Oleate	7.5	9.4	7:1
8. Chol. Erucyl Carbonate	7.45	8.7	1.2:1
9. Chol. Geranyl Carbonate	7.45	9.0	Very low
10. Chol. Myristate	7.44	9.3	1.8:1
11. 3 Me Vai *	7.47	8.5	Very low
12. Sitosteryl Oleate	7.47	8.6	Very low

Detailed measurements of the angular light-scattering distribution have revealed that, with the illuminating source normal to the cell surface, maximum scattering generally occurs between 40 and 50 deg from the incidence angle rather than the 30-deg angle used in these experiments. At the maximum scattering angle, the reflectivity of some samples would be much higher than the value measured at 30 deg and indicated in Table VII.

D. CONTRAST RATIO

For practical purposes, the contrast ratio of our storage type unit is defined as the light intensity in the scattering state (after the low-frequency "write" signal has been removed) divided by the light intensity in the clear state (after the high-frequency "erase" signal has been removed). Obviously, at certain relative angles between the incident and reflected (or transmitted) light, contrast ratios much less than unity (or negative contrast ratios) are possible. Since scattering intensity is a function of the magnitude and frequency of the applied electric field, it was necessary to define the conditions under which the contrast ratios were measured. Higher contrast ratios were possible under field "on" conditions since both the scattering texture and transparency of these mixtures could be improved by maintaining an appropriate ("write" or "erase") ac addressing signal.

The contrast of units fabricated with various mixtures in the nematic-cholesteryl oleate system generally ranged between 3:1 and 8:1, the highest ratio occurring for units made with a mixture containing approximately 7.5% of the cholesteryl oleate component. This mixture generally was more scattering under storage conditions and relatively transparent in its quiescent (clear) state. None of the other nematic-cholesteric mixtures investigated were superior in contrast ratio or comparable in terms of other electro-optic characteristics.

It should be noted here again that, by optimizing the measurement parameters, more impressive values of contrast ratio (greater than 10:1) were possible. The measurement technique used (to evaluate materials) could be considered more qualitative than quantitative but the reported contrast ratios are more representative of practical values that would be discernible to the average observer of a large-area display. Since viewing requirements of some display systems may not be especially critical, it is conceivable that further contrast improvements may not be necessary and, in fact, may allow a suitable "trade-off" to compromise other potentially important performance characteristics. For instance, some cholesteric-nematic mixtures can be operated by considerably reduced electric fields at the expense of contrast ratio and storage capabilities, thus offering the possibility of multiplexed operation.

E. STATIC ELECTRO-OPTIC CHARACTERISTICS

One of the extremely desirable aspects of a large-scale, matrix-addressed display is the presence of a coincidence threshold, i.e., the behavior of the display medium such that signals below a given level result in no response but signals of twice the threshold level result in an "on" condition of the display. In certain classes of nematic liquid crystals operated in the dynamic scattering mode no such coincidence threshold exists and scattering increases with voltage above a minimum threshold (~ 6 to 8 V) until saturation sets in at about 35 V. Measurements have been made to determine the changes that occur in such nematic systems by the addition of cholesteric material.

A plot of threshold field vs. percent cholesteric component is shown in Figure 8. For all the compositions measured, the field required to produce the onset of scattering (threshold) increased with increasing cholesteric content. At low ac frequencies within the "write" frequency range, it is likely that slightly higher electric fields would be necessary to yield similar results. This has been reported elsewhere [16].

The experimental data presented in Figure 9 show the scattering (reflective mode) behavior of typical half-mil-thick RSM cells as a function of steady-state excitation voltage. During the course of these tests made with cholesteryl oleate-nematic mixtures, a number of response features relevant to the objectives of our materials synthetic effort were consistently observed:

- (1) A 2% cholesteryl oleate-nematic mixture behaved similar to a nematic LC cell operated in the dynamic scattering mode. Between a threshold voltage of 2 and 3 V and a saturation level of 10 to 15 V a gradual increase in scattering (reflectivity) was observed. Removal of the dc voltage required to produce maximum reflection (15 to 20 V) resulted in rapid deterioration of the scattering texture — the unit became very nearly transparent in a matter of minutes.
- (2) Cells made of 5 to 15% cholesteryl oleate-nematic mixtures did indeed exhibit a sharp coincidence threshold. The voltages needed for maximum reflectivity were less than twice the voltages measured at the onset (threshold) of the light-scattering process. A further increase in voltage beyond the reflectivity maximum reduced the amount of scattered light reflected back to the photodetector.
- (3) The electro-optic properties of a limited number of test units fabricated with

materials containing greater than 2% of the cholesteric component were characteristic of the pure cholesteryl ester in that they showed higher threshold voltages and required higher rms "erase" signals.

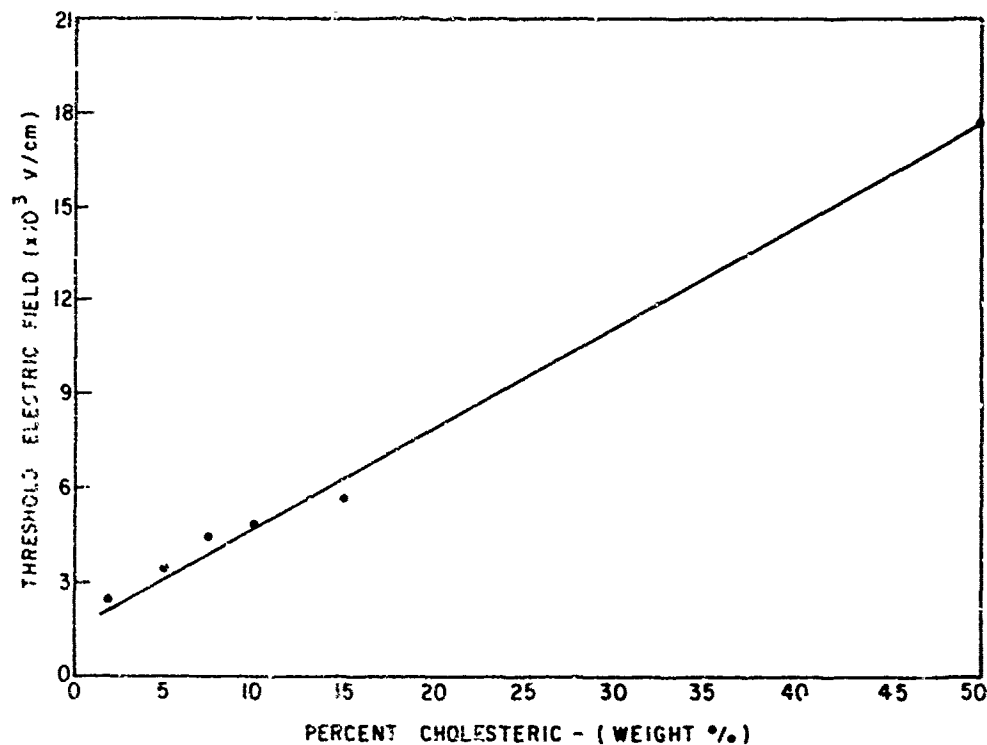


Figure 8. Threshold field as a function of cholesteryl oleate content.

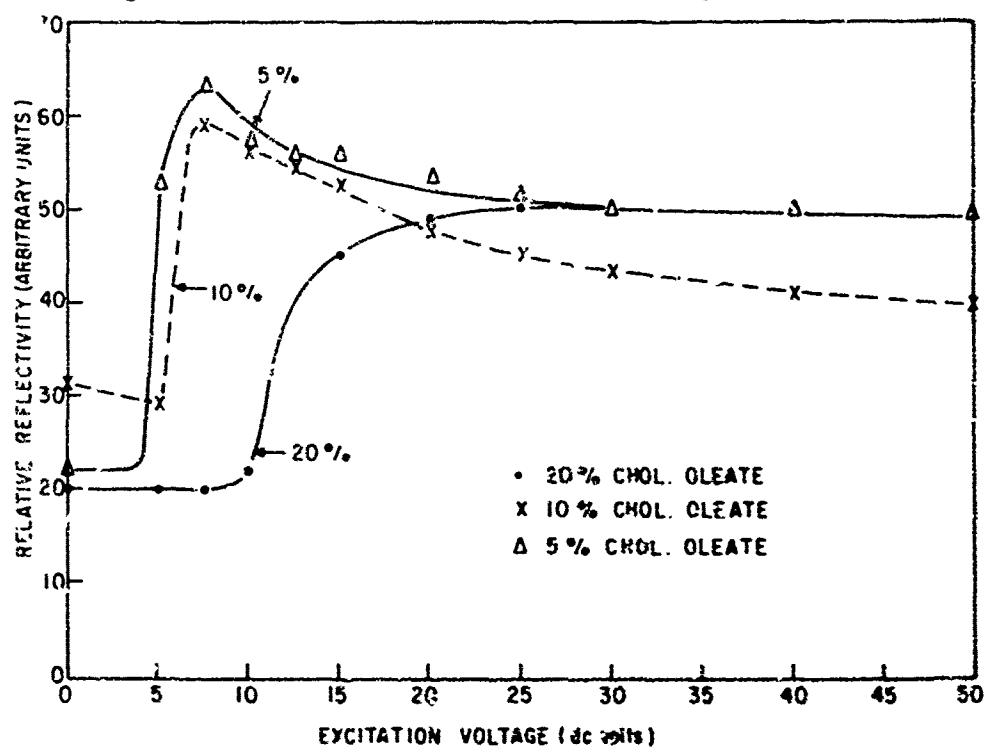


Figure 9. Static electro-optic response of reflective storage cells.

The data presented above provided a useful diagnostic means for understanding the mechanism of the storage system and for determining electro-optic characteristics as affected by the cholesteric content of the mixture. It was often necessary to maintain steady-state field conditions for several seconds before an electro-optic equilibrium was observed. For utility in real-time or "rapid update" display systems where long time storage is not of primary importance, the transient or dynamic electro-optic properties of these materials are likely to be more significant.

F. DYNAMIC ELECTRO-OPTIC CHARACTERISTICS

In a dynamic display system utilizing the storage capabilities of appropriate cholesteric-nematic mixtures, the speed of optical response to a particular excitation voltage is likely to be an important parameter. To facilitate further discussion it is necessary to define and elaborate on the terms "writing" and "erasure" speed as applied to the operating characteristics of a typical storage device. Assuming a reference scale where the scattered light intensity in the clear state is equal to zero, then "writing" speed refers to the time interval which elapses from the moment the dc or low-frequency ac voltage is applied until the scattering state has reached 90% of its field "on" value. Similarly, "erasure" speed refers to the time interval elapsed from the moment the high-frequency "erasure" field is applied until the scattering has been reduced to 10% of its field "off" (storage state) value.

Perhaps a better understanding of these definitions and an appreciation of some of the experimental problems involved in this type of measurement can be acquired by referring to the illustration in Figure 10. The electro optic properties of the cell chosen for this illustration are representative of the unique operating characteristics of those units fabricated with between 5 and 15% of the cholesteric component in our nematic host (NH-1).

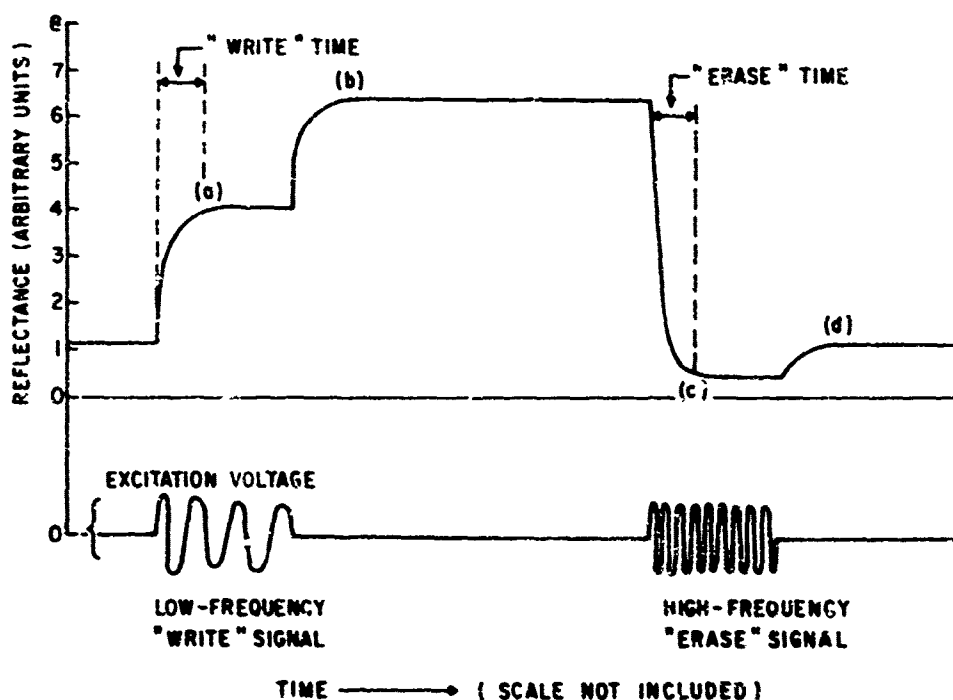


Figure 10. Dynamic electro-optic response of typical reflective storage cell.

No time scale has been included in this plot since the four time constants shown have significantly different values and because both "writing" and "erasure" speeds are vitally dependent on the frequency and magnitude of the addressing signals. For similar reasons a scale for the applied excitation voltage has not been included. The information contained in this graph merely illustrates the different values of scattering that result during high- and low-frequency "on" and "off" conditions. The letter designations on the reflectivity curve correspond to steady-state values measured

- (a) — with a low-frequency field maintained across the test unit,
- (b) — after the "write" signal has been turned "off",
- (c) — some time interval after the high-frequency excitation voltage has been turned "on", and
- (d) — after the "erase" field has been turned "off".

The specific electro-optic response characteristics of a test cell fabricated with 7.43% cholesterol oleate-nematic mixture are shown below.

Table VIII
Electro-Optic Response Characteristics

	Addressing Condition		Reflectivity (arb. units)
Write	60 Hz (100 volts rms)	"on"	40
		"off"	64
Erase	6 kHz (100 volts rms)	"on"	5.9
		"off"	11.8

The speed-of-response properties of all the tested units were measured using a "write" frequency of 60 Hz at 100 V (rms) and an erase signal of 6 kHz at the same rms amplitude. These values of frequency and voltage were chosen mostly as a matter of convenience and, although other frequency-voltage combinations may yield improved response characteristics, these measurements did allow a comparative means for materials evaluation. The cumulative results of these tests indicated that the dynamic electro-optic response of the cholesteric-nematic mixtures investigated could easily be categorized into three general classes (although the properties probably vary continuously as the percentage of cholesteric is varied):

- (1) "Writing" speeds of 5 to 10 msec and "erasure" speeds of 20 to 25 msec were measured on those units fabricated with 2% or less cholesterol oleate-nematic mixture. This behavior is similar to the dynamic scattering mode of operation in pure nematic liquid crystals.
- (2) Cells made of 5 to 20% cholesteric-nematic mixtures respond to "write" signals in 2 to 8 msec and can be "erased" in 0.5 to 1.0 sec. Very little difference in speed of response was noted within the specified range of cholesteric composition.
- (3) Greater than ~ 20% cholesteric content resulted in a cholesteric-dominated electro-optic response. That is, scattering saturation had not been achieved at 100 V, color changes were readily apparent, and voltages greater than 200 V (ac or dc) were required to revert the units back to their original clear state.

Figure 11 shows the response times of several nematic host materials as a function of applied dc voltage. More detailed measurements of response time vs. voltage and frequency were not made because of the difficulty in interpreting the optical response characteristics and because writing and erasure speeds were also found to be dependent on sample thickness and temperature.

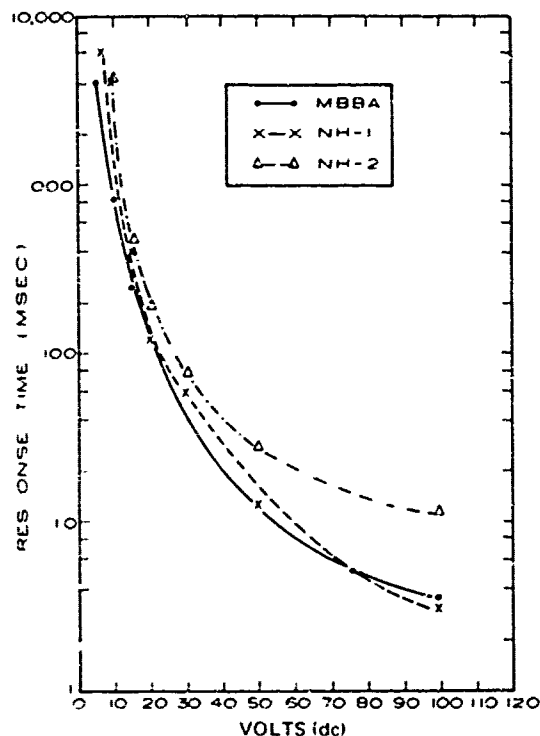


Figure 11. Response time as a function of voltage for three different nematic host materials.

G. STORAGE PROPERTIES

One of the important properties required of the material combinations under investigation was their ability to retain their scattering texture over a long period of time with no maintaining power. Most of the tested samples faded gradually after the removal of the excitation voltage but the "relaxation" process proceeded at different rates for the various cholesteric-nematic combinations. There were three principal types of failure involved in the attrition of test units stored for periods ranging from a few hours to four months:

- (1) reduction in reflectivity and/or contrast ratio,
- (2) development of an X-pattern in the surface texture, and
- (3) crystallization of the cholesteric-nematic mixture.

Table IX summarizes the storage behavior of some of the cholesteric-nematic mixtures investigated. Life test data were recorded only in terms of reflectivity, contrast ratio, and visual appearance. Storage life termination due to crystallization of the liquid crystal mixture occurred only in samples containing much more than 20% of the cholesteryl component.

None of the experimental cells used for storage life testing were encapsulated nor were they subjected to environmental testing under controlled ambient conditions. From the accumulated data, storage life appears to be a lesser problem area. A summary of results for unsealed cells stored at room temperature (NH-1 nematic component) indicates a storage time expectancy of

- (1) 60-90 days for 7.5% cholesteryl oleate component, and
- (2) 90-120 days for 20% cholesteryl chloride component.

Table IX
Storage Behavior of Cholesteric-Nematic Mixtures

% Cholesteryl Oleate	Duration of Test	Comments	Reason for Termination of Test
7.5	78 days	Unit became very nearly transparent. Remeasurement of dynamic E-O response shows same results as initially.	Reflectivity and contrast too low. Texture almost clear.
10	20 days	Reflectivity and texture nonuniform.	Deterioration of texture and appearance.
15	50 days	Undesirable formation of patterns in light-scattering texture.	Overall reduction in reflectivity and poor cosmetic appearance.
20	42 days	X-pattern has developed and edges of cell have poor appearance.	Deterioration of texture and appearance.
% Cholesteryl Chloride			
20	121 days	Fairly uniform appearance but reflectivity is decreasing.	
% Cholesteryl Erucyl Carbonate			
7.15	15 minutes	Became nearly clear in about 15 minutes.	Poor storage. Contrast reduced by one-half in just a few minutes.
% Cholesteryl 2-Methoxy Ethoxy Carbonate			
7.11	~ 12 hours	Temperature behavior of this material was good. Unit operates well up to 60°C.	Scattering texture of "stored" state was retained for less than 24 hours.

At elevated temperatures storage properties were adversely affected, and near the isotropic temperature the stored state could be retained for only a few minutes.

In order to estimate lifetime potential under dynamic operating conditions, a number of cholesteric-nematic mixtures were programmed for periodic cycling between the "stored" and "erased" state. All of the measured cells were subjected to the following test conditions:

- (1) one second "write" field "on" (90 V dc),
- (2) two seconds "write" field "off",
- (3) one second "erase" field "on" (90 V rms, 6 kHz), and
- (4) two seconds "erase" field "off".

Cells were considered to have failed the cycling test if a significant reduction in contrast ratio occurred or if an objectionable deterioration in scattering texture appeared. Unsealed cells previously used for static storage life studies failed initial dynamic testing in less than 1,000 cycles due to the formation of gas bubbles throughout the active cell area and especially at the periphery. However, the active life period of freshly prepared samples, vacuum evacuated to remove gas bubbles trapped during the cell fabrication process, has been extended appreciably. After 8,000 cycles only a slight cosmetic deterioration along the cell edges was observed. Hermetic sealing of the cell structure, a technique which was developed at RCA, is expected to further increase operational lifetime.

At the present time there is no evidence to indicate that sequential cycling between "write" and "erase" excitation fields adversely affects operational lifetime as usually determined by steady-state field conditions. No differences in dynamic behavior were found for cholesteryl oleate concentrations of 5 to 15% in NH-1. In fact, the contrast ratio of one test unit fabricated with 5% cholesteryl oleate - NH-1 increased after 8,000 cycles of operation due to improved transparency of the cell after the "erase" signal had been removed.

Life studies were also made on cells designed with a matrix type electrode pattern to determine static storage effects on adjacent segments located in close proximity to a sequentially operated active element. This work was essential if we were to design a state-of-the-art display which illustrates a practical application of the storage effect.

Figure 12 is a drawing of a test cell designed with a nine-element matrix-type electrode pattern. The optical condition of each discrete element is also shown. To simulate an addressing scheme where the desired display information is in digital format, two of the nine segments in the pattern were sequentially activated using excitation signals and relaxation periods of

- (1) "Write" - 90 V dc for 1 second, relax for 2 seconds, and
- (2) "Erase" - 90 V at 6 kHz for 1 second, relax for 2 seconds.

The static lifetime of inactive "stored" segments adjacent to inactive "clear" segments was about 30 days. However, no apparent optical deterioration occurred in *any* of the unexcited elements located adjacent to the dynamically cycled segments even after 15,900 cycles of operation. Termination of these tests was dictated by the failure of the electronically addressed elements due to the formation of bubbles along the active cell periphery. The results of these tests indicate that proximity effects between "stored", "clear", and active adjacent elements will not be limiting factors in the design of a state-of-the-art display using our storage-type liquid crystal materials.

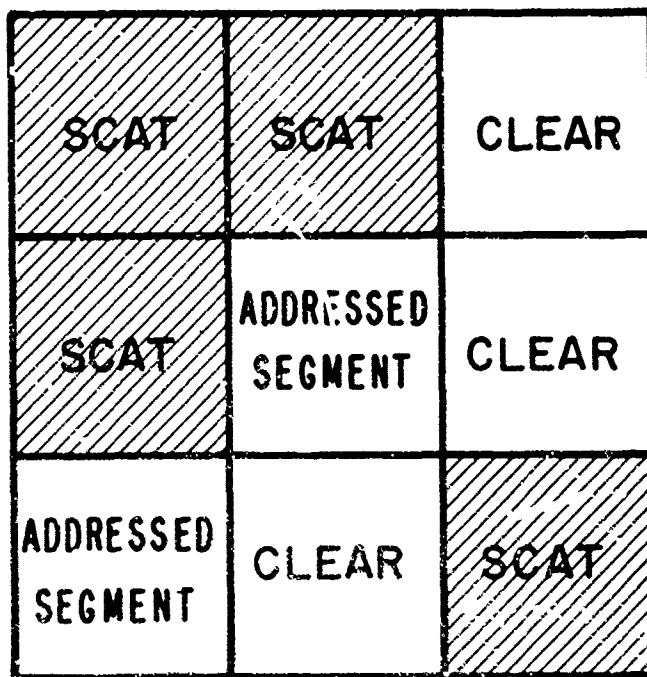


Figure 12. Segmented storage cell (top view).

H. DEVICE THICKNESS

A brief examination of electro-optic properties as a function of cell thickness was made to determine an optimum thickness for larger area (10 cm x 10 cm) display cells. At 0.25-mil electrode spacing, the necessary high electric fields were conducive to excessive short-circuiting. Poor contrast ratios and slow response speeds were observed for cell thickness greater than 1.0 mil. From these limited tests it appears that a 0.5-mil separation between the parallel conducting glass plates is a satisfactory compromise between contrast, uniformity, speed of response, and addressing requirements.

I. TEMPERATURE EFFECTS

Several parallel-plate test cells using various mixtures from the cholesteryl-nematic systems were fabricated and their electro-optic properties measured as a function of operating temperature. Though variations in temperature dependence were found to occur for different compositions, the behavior of all the tested units could be generalized as follows:

- (1) Abrupt changes in temperature caused drastic changes in the texture of the stored state. At high heating (or cooling) rates, partial erasure of the stored, scattering texture occurred. More specifically, nonisothermal conditions due to temperature gradients across the test cell allowed fluid motion of the liquid crystal material to partially convert the focal-conic texture to the clear planar state.

- (2) At a constant temperature ($\pm 2^\circ\text{C}$) within the liquid crystalline range of the material, cells could be operated normally in both the storage and erase modes. In fact, some improvements in contrast ratio and response speed, and a decrease in threshold voltage were noted up to temperatures of 65°C . However, as the temperature was increased closer to the N-L transition point, light scattering and storage properties were adversely affected.
- (3) Near the isotropic temperature of the mixtures under test, the scattering properties and contrast ratios were significantly reduced and the focal-conic texture of the stored state was retained for only a matter of minutes.
- (4) Life measurements at elevated temperatures indicate satisfactory storage up to 24 hours at temperatures near 50°C (NH-1).

A more extended study of temperature effects was not undertaken because of the various parameters (i.e., nematic range of host material, the cholesteric component and its content in the mixture) affecting the transition temperatures of the material combinations under test.

J. CAPACITANCE MEASUREMENTS

Capacitance measurements as a function of dc voltage and cell thickness were made in order to determine the dielectric anisotropy of the mixture 7.5% cholesteryl oleate in nematic host NH-1. Spacing between the parallel-plate electrodes was varied between 0.25 mil and 2.0 mils for four different cells containing the selected mixture, and the dielectric constant was calculated at each thickness. All of the capacitance data were obtained using a Boonton capacitance bridge having an ac test signal of 100 kHz at ~ 90 mV (rms). Reliable and reproducible results were obtained under the following conditions:

- (1) Initial measurement was made at zero dc bias with the test cell in its clear (planar texture) state.
- (2) The capacitance was measured as a function of dc voltage until the scattering texture was readily apparent.
- (3) The dc voltage was removed, and the capacitance of the (stored) focal-conic texture was measured.

For this particular cholesteric-nematic mixture, the average dielectric constant was calculated to be 4.9 for the focal-conic texture and 5.8 for the planar texture. Intermediate values of dielectric constant were recorded with a dc bias voltage (above threshold) applied to the test cell. This 20% change in dielectric constant is typical of the anisotropy variation for nematic compound similar to the NH-1 nematic host used in our present storage material.

K. LIGHT-SCATTERING CHARACTERISTICS

To optimize display-related parameters and to obtain a better understanding of the light scattering characteristics of a reflective storage cell in its "scattering" and "clear" states a series of measurements was made. Figure 13 shows the angular notations used in these measurements and some of the results for a 0.5-mil parallel-plate cell containing 5% cholesteryl oleate in NH-1. Both the incident light source and the cell under test were allowed angular movement in one plane — either mutually or independently. The brightness of the cell was recorded with the photodetector in

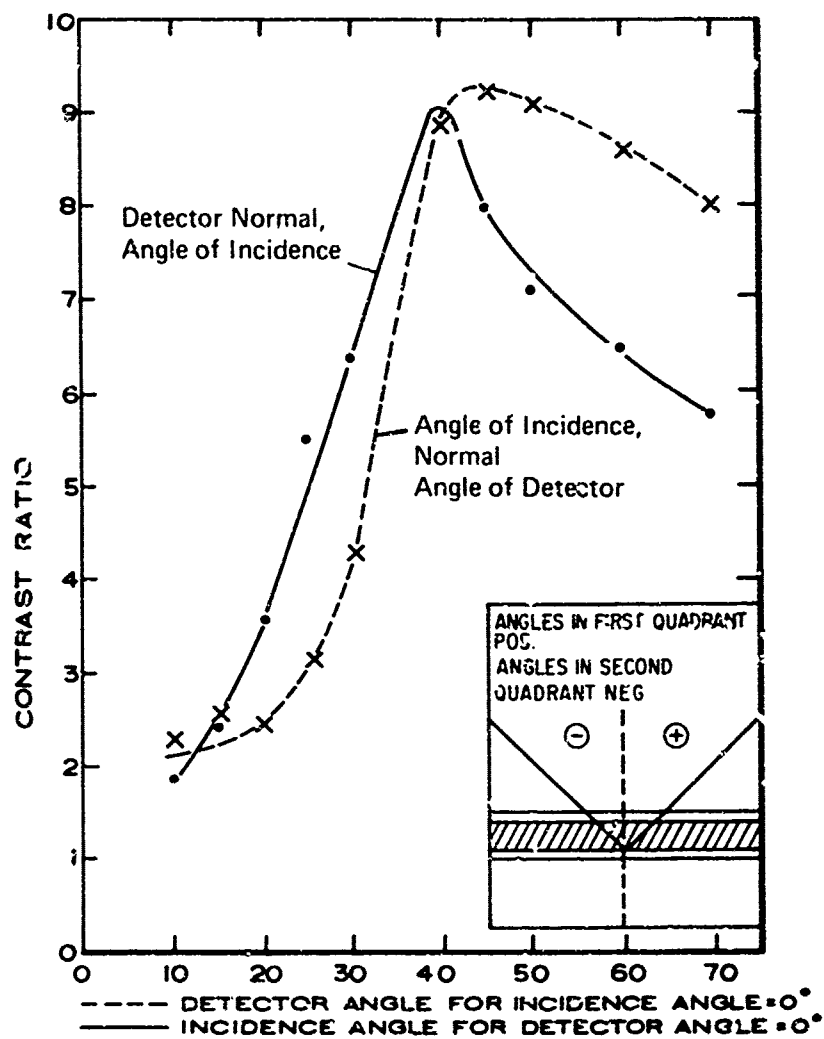


Figure 13. Contrast ratio as a function of incidence and reflection angles.

a fixed position. Based upon the relative brightness and contrast ratios at various angles of incidence and reflection, the following conclusions can be made:

- (1) When the angle of incidence is normal to the cell surface, maximum contrast occurs at approximately 45-deg angular displacement of the photodetector. With the photodetector normal to the cell surface, the contrast ratio peaks abruptly at an angle of incidence of ~ 40 deg
- (2) Obviously, maximum brightness occurs in both the "scattering" and "clear" states at the specularly reflecting angle. This condition of incidence and reflection angle being equal does not serve any useful purpose other than to demonstrate a polarity reversal of the contrast ratio; i.e., the light reaching the detector is greater when the liquid crystal cell is "clear" rather than in its scattering texture.

These characteristics represent the general behavior of a specific cholesteric-nematic mixture operating in the reflective storage mode. More detailed studies of the transmitted light-scattering properties as a function of material composition and cell thickness were made and are discussed separately in this report (Section IV).

L. MATERIAL RESISTIVITY

To determine if the cholesteric component in our nematic-cholesteric mixtures produced significant electrical conductivity changes, the dc resistance of cholesteryl oleate and cholesteryl chloride in NH-1 was measured. The steady-state dc resistivity as a function of cholesteric content is shown in Figure 14. From the vast differences in resistance values, it is apparent that the purity, type, and content of the cholesteric component did indeed affect the resistivity of the liquid crystal mixtures.

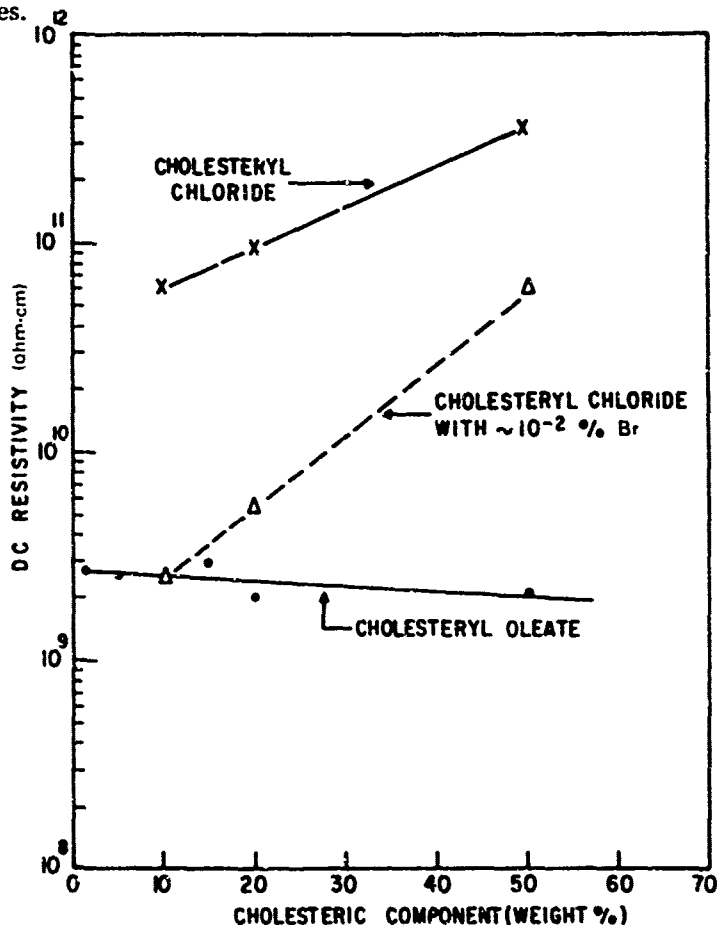


Figure 14. DC resistivity as a function of cholesteric components.

It was possible to reduce the resistivity of the cholesteryl chloride — NH-1 mixtures by addition of $\sim 10^{-2}$ % hexadecylpyridinium bromide, but no significant differences or improvements in device performance were noted. However, more recent devices made with purified cholesteryl oleate material were much more resistive than previous mixtures having the same percentage content, and these units exhibited poorer electro-optic properties. Current experimental studies suggest the likelihood of a specific materials resistivity range for optimum device performance. Although these data are still incomplete, it appears that materials having a bulk resistivity of less than 10^{10} ohm-cm exhibit response characteristics superior to devices made with higher resistivity materials.

SECTION IV

LIGHT-SCATTERING BEHAVIOR

Quantitative measurements of light scattering are desirable for comparing various materials and for optimizing the design of storage cells. The absolute value of scattered light intensity at a given viewing angle determines the brightness and contrast ratio that can be obtained with a certain material. The thickness and angle dependences will influence the particular cell design. Such measurements have been made in cholesteryl oleate — NH-1 mixtures.

In the nonscattering state the material takes on the *planar texture* [4]. The helical axis of the cholesteric structure lies perpendicular to the plane of the electrodes, while the molecules lie parallel to that plane. Usually no preferential direction is established within this plane and one must assume that the molecular axes are randomly oriented in the plane. The orientation must change smoothly from point to point as these fluctuations cannot be observed under the microscope.

The clear state is obtained by the application of a high-frequency field. The frequency is too high to effect any movement of charge so that the field acts only on the dielectric properties of the liquid. The dielectric anisotropy of the molecules is negative, and they align perpendicular to the field, i.e., in a plane parallel to the electrodes. The field itself does not introduce any preferred direction within that plane, so that the orientation will depend mainly on the wall forces.

When a low-frequency or dc field is applied to the clear cell it becomes highly scattering, despite the fact that the dielectric forces alone tend to keep the molecules aligned in the planar texture. This is identical to the situation in nematic materials of negative dielectric anisotropy. The light scattering in this *dynamic scattering mode* [18] (DSM) is caused by turbulent flow of liquid due to movements of charge through the nematic material. The light-scattering properties of the storage material are expected to be similar to those of the DSM in nematic materials.

When the field is removed, and liquid motion ceases, another stable cholesteric phase is formed. Because of the "memory" of the turbulent condition, the helical axis in this texture is oriented in different directions in different regions. This appears to be the well-known *focal-conic texture* [4]. The liquid is at rest but scattering of light takes place because of constant variations in the direction of the "crystalline axis".

A. EXPERIMENTAL

The experimental arrangement for measuring the scattering parameters is shown in Figure 15. The light source is a microscope lamp, collimated so that the light incident on the cell has an angular spread of about 5 deg. Both the angle of incidence (θ) and the angle of measurement (ϕ) could be varied but light propagating outside the plane of the diagram was not considered. For some of the investigations with monochromatic light a He-Ne laser was used, and the incident light was then completely collimated.

The scattered light was measured in two different ways. In one method only one part of the cell was illuminated, and the light (scattered into a well-defined solid angle) was measured with a photomultiplier. This produced a value which was easy to interpret physically. In the

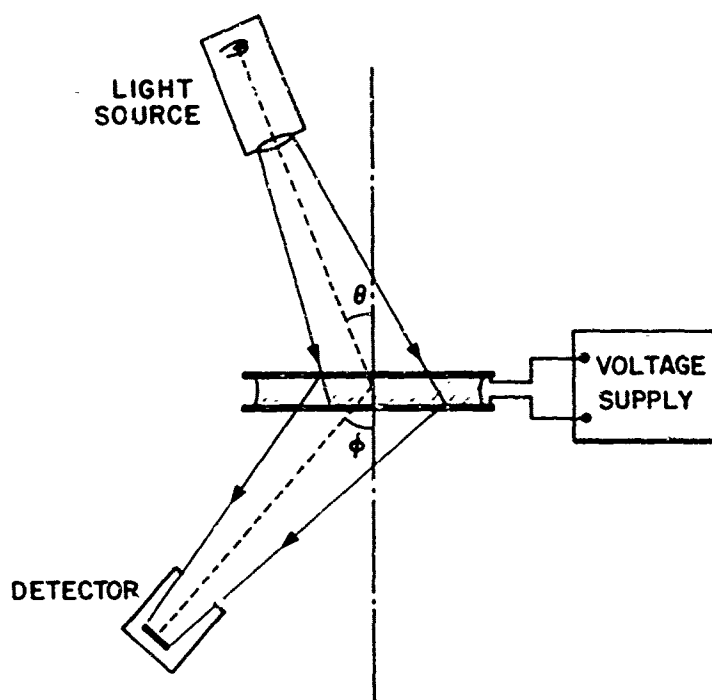


Figure 15. Experimental arrangement for measuring light scattering of liquid crystal cells.

other technique the entire cell was illuminated and the brightness measured with a spot brightness meter. This number represents the quantity that a viewer would observe in an actual display. It is related to the first quantity in the following way. The incident light intensity is proportional to $\cos\theta$. The brightness meter measures the light impinging on it from a fixed solid angle. As the distance to the cell is kept constant the cell area subtended by the solid angle must vary as $1/\cos\phi$. Consequently, the reading of the brightness meter will be $\cos\theta/\cos\phi$ times the value of the photomultiplier reading.

In making the measurements, care was taken to obtain reproducible results. Cells had to be prepared by a standard procedure, and the voltages had to be applied in the same magnitude and in the same time sequence. In this manner the values of scattered-light intensity in the DSM and in the storage state could be reproduced reliably. There tends to be somewhat more fluctuation in the attenuated direct beam.

A typical curve of light scattering as a function of viewing angle is shown in Figure 16 for one cell in three different conditions. The clear state still shows a substantial amount of scattering which is the reason for the relatively low contrast ratios of these cells. The degree of this scattering was quite variable from cell to cell. It may be related to the exact treatment of the wall surfaces, although we have not been able to demonstrate this conclusively. The scattering was considerably reduced during the erase cycle with the high-frequency field, and the planar texture appeared almost transparent [19]. When the field was removed, however, some misalignment took place with the molecules rotating out of the plane of the cell. The reason for this is not understood at present.

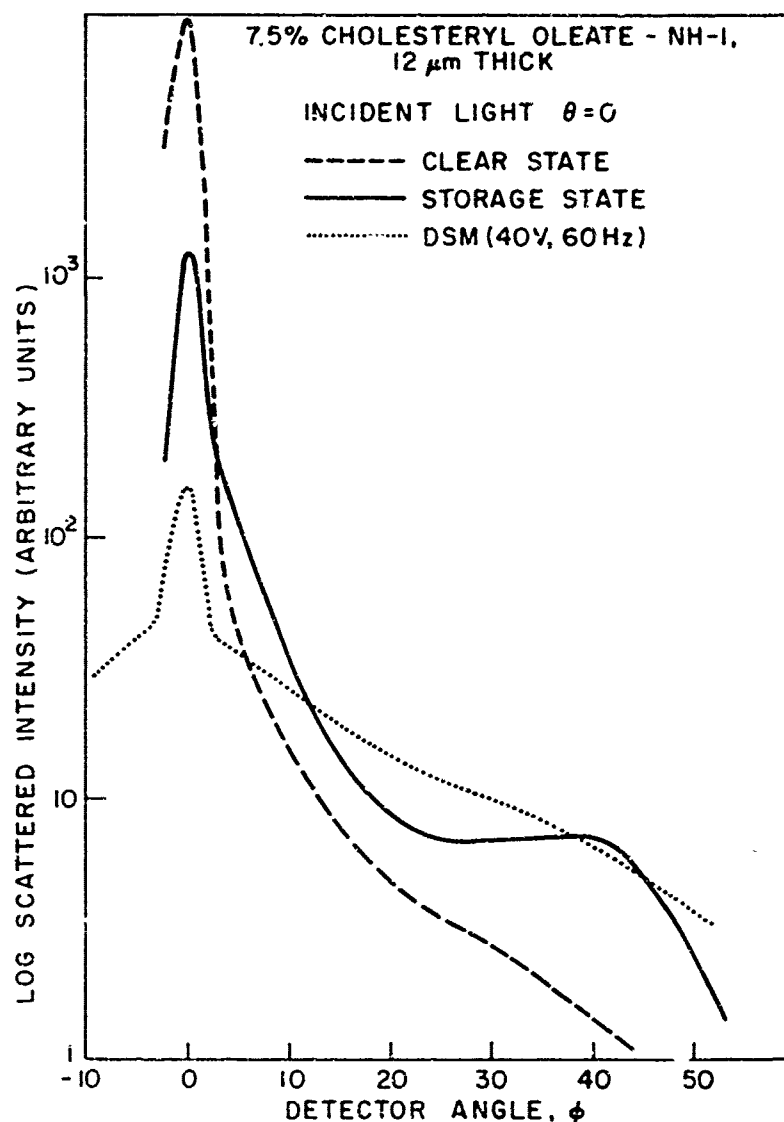


Figure 16. Scattering intensity vs. detector angle.

When a low-frequency electric field was applied to the cells, an electro-hydrodynamic instability set in at a well-defined threshold voltage. At higher voltages the liquid flow became turbulent. The typical scattering curve in Figure 16 shows a strongly attenuated unscattered beam and a slowly and monotonically decreasing scattering behavior. The characteristic is the same as that observed in the DSM of nematic materials with negative dielectric anisotropy. This is also true of the dependence on voltage, angle, and sample thickness. As an example the voltage dependence of the DSM in a storage material is shown in Figure 17.

When the voltage was removed and the turbulent motion ceased the scattering focal-conic texture was produced. Figure 16 demonstrated that the amount of light scattered at a given angle is similar to the DSM case, but there are differences in detail. There appear to be three contributions to the transmitted light: the attenuated direct beam, a part which decreases monotonically with scattering angle and a narrow band located between 25 and 55 deg.

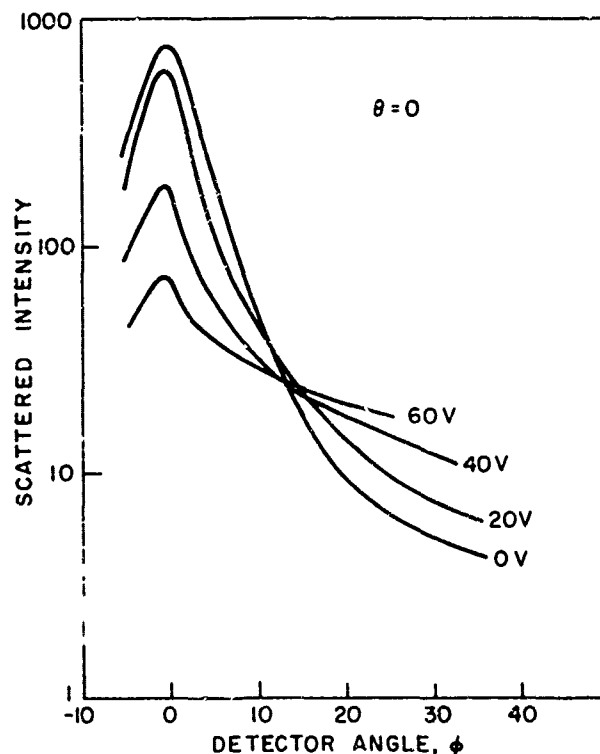


Figure 17. Voltage dependence of scattered light intensity.

The central peak has approximately the same angular distribution as the incoming beam and mainly represents the attenuation of that beam due to scattering. The broad peak at larger angles is due to Bragg scattering of the periodic structure of the cholesteric material. The repeat distance of the structure is half the pitch p of the helix since two planes perpendicular to the helical axis separated by $p/2$ contain molecules oriented in the same direction (one cannot distinguish between the two possible orientations along the molecular axis). In the focal-conic texture the helical axis direction is continuously changing from point to point. On the scale of microns, such as is used in storage cells, this amounts to a random distribution of orientation directions. The texture can then be thought to be the analog of a polycrystalline material or a crystal powder, and the Bragg scattering is similar to a powder x-ray diffraction pattern. The diffraction rings appear because there are always some "crystallites" oriented so as to fulfill the Bragg scattering equations:

$$\lambda' = (p/2) 2 \sin (\gamma/2) \quad (1)$$

as shown in Figure 18. Here λ' is the wavelength in the medium ($\lambda' = \lambda/n$), and θ' and ϕ' are the interior angles, related to θ and ϕ by Snell's law, $\gamma = \theta' + \phi'$. The third contribution to the scattered energy, which has a monotonic dependence on angle, must be due to the random distribution of "domain" sizes and orientations of the focal-conic texture with their concomitant variations in refractive index. The effect is qualitatively similar to the scattering behavior of the DSM except in the latter case the scattering due to the randomly oriented and constantly changing turbulent vortices is considerably stronger and drops off more slowly with angle.

It should be noted, at this point, that both the DSM and the clear planar texture sometimes appear to have a small amount of Bragg scattering. For the planar texture this means that

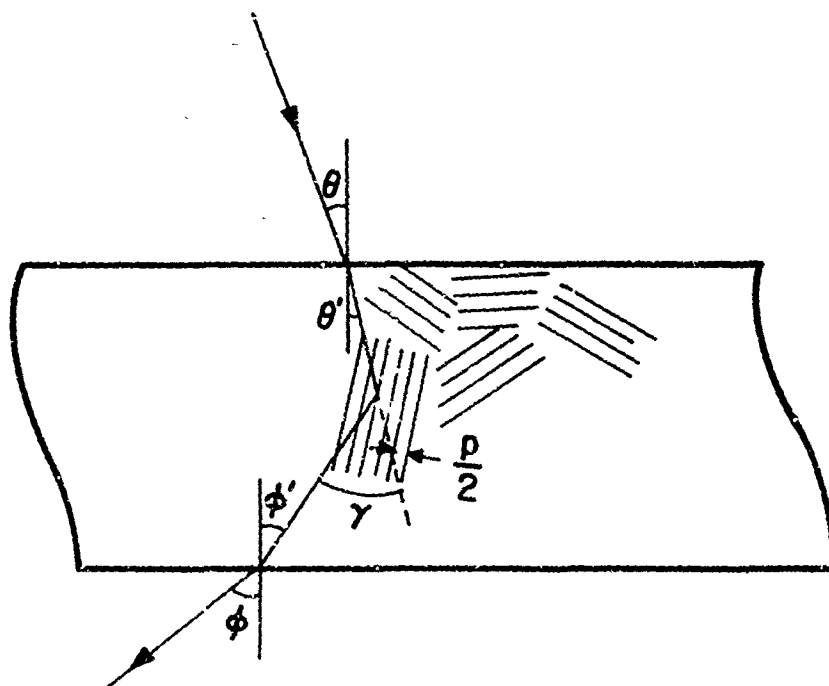


Figure 18. Schematic designation of Bragg scattering angles in the focal-conic texture.

the misorientation mentioned must include some tilt in the helical axis as well as possible distortions at the walls and out of planes parallel to the walls. The flow in the DSM must be sufficiently fast and turbulent so that the helical ordering of the cholesteric phase is almost completely disrupted.

A number of tests were made to compare materials of different compositions. Some results for the storage state are shown in Figure 19. The curves are very similar in magnitude. However, only the two intermediate concentrations show the Bragg scattering peak. It has also been observed at a similar angle in a 20% mixture. By using a monochromatic He-Ne laser, accurate values of the peak position could be obtained. Values of $p/2$ derived by Eq. (1) average $0.8 \mu\text{m}$ with little variation over this concentration range. At lower values of concentration a larger pitch and smaller scattering might be expected, but this was not observed. It may be that the value of $p/2$ is now of the same order as the "domain" size of the focal-conic texture so that there are not enough planes of equal orientation parallel to each other.

When looking at this texture with monochromatic light other diffraction effects are also occasionally observed, corresponding to spacings of 3 to $10 \mu\text{m}$. These can also be seen under the microscope as domain-like structures of uniform spacing. They may be part of the typical focal-conic texture arrangement in thin cells.

For the optimum design of storage cells it is important to know the thickness dependence of the various parameters. The scattering intensity in the storage state is shown in Figure 19 for three cells of different thickness. The intensity and angular dependence of the scattered light vary only slightly among the three samples, a rather surprising result. It can be demonstrated in a more quantitative way by considering the attenuation of the direct beam. The average ratio of transmitted to incident beam obtained from Figure 20 and other data are shown in Table X. If the scattering medium were uniform one would expect the attenuation to vary exponentially with

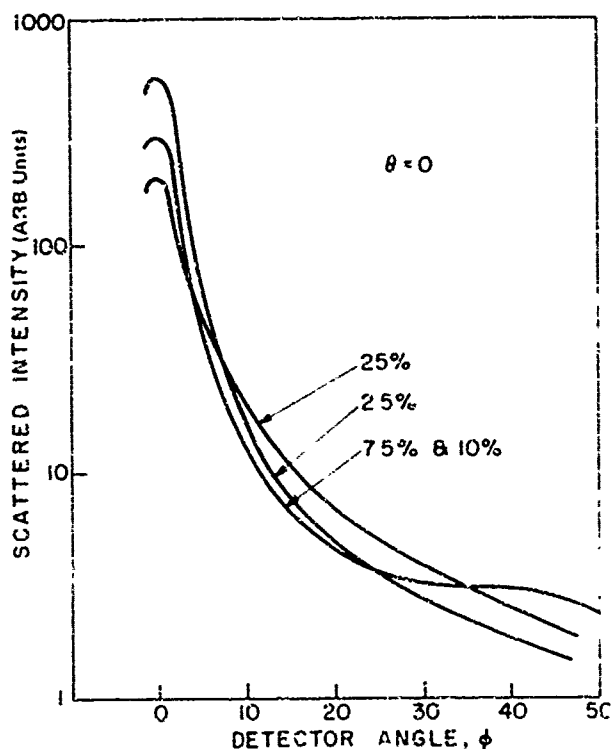


Figure 19. Angular light scattering intensity as a function of cholesterol oleate content.

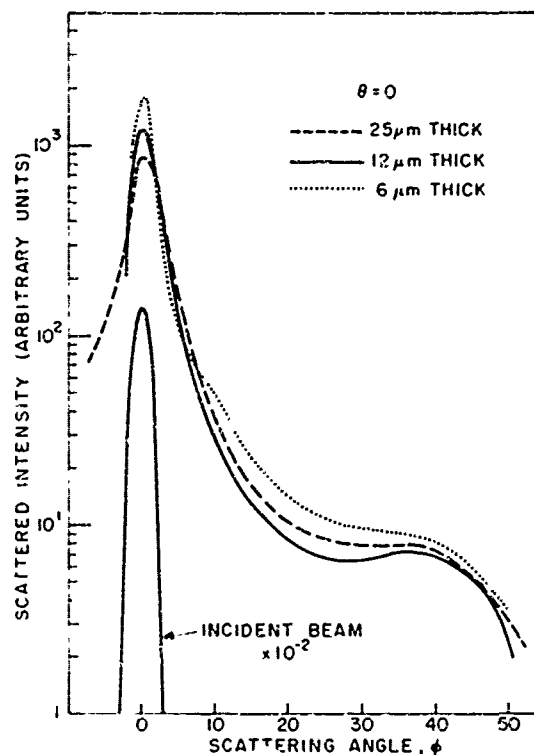


Figure 20. Angular light scattering intensity as a function of cell thickness.

thickness (at those values of attenuation the fraction of light scattered back into the direct beam can be completely neglected), leading to an attenuation coefficient

$$\alpha = \frac{1}{d} \ln(I_0/I) \quad (2)$$

The calculated values of α are shown in Table X. Since they vary considerably the assumption of uniform scattering must be incorrect.

To check the validity of our assumptions in the considerations of attenuation we measured a number of combinations of two storage cells on top of each other, or effectively in series. An example is shown in Figure 21. For the model used the attenuation of the series combination should be equal to the product of the attenuations of the individual cells. One 6- μ m cell attenuates the beam about 8 dB (Table X), while two cells cause 17-dB attenuation, about as expected.

Table X
Attenuation of Direct Beam in Storage Cells
of Various Thicknesses in the Storage State

	A	B	C
Cell Thickness	25 μ m	12 μ m	6 μ m
Attenuation Ratio	0.038	0.085	0.15
Logarithm (dB)	14.2	10.8	8.1
α	0.13 μ m ⁻¹	0.21 μ m ⁻¹	0.31 μ m ⁻¹

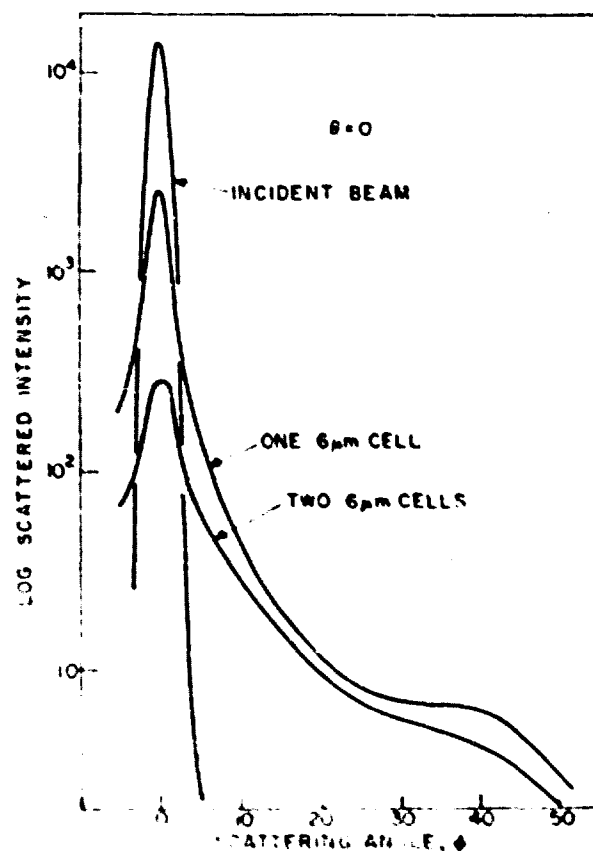


Figure 21. Scattering properties of two cells in series compared with a single cell.

To understand the thickness dependence of the scattering in the storage mode we must first discuss the dynamic scattering mode, from which it is derived. One finds in both the nematic and storage materials that the scattering in the DSM is quite independent of thickness at a given voltage. There are two considerations that may contribute to the explanation of this effect. First, the fact that the electric field, at a given voltage, is higher in thin cells, produces higher liquid velocity and increased turbulence which may cause more scattering per unit volume, compensating for the reduction of the volume with thickness. The other possibility is that the flow is relatively uniform in the interior of the cells, that most of the turbulence and scattering is in layers near the surface which have the same properties for all thicknesses. If one assumes that the focal-conic texture, which forms after the flow has ended, has a structure partially determined by the flow patterns, then the second possibility would appear to be dominating. There is the additional experimental information that the structure of the focal-conic texture does not depend strongly on the voltage applied in the DSM above a certain minimum. This could still be compatible with the notion that most of the structural variation takes place near the surface of the cell.

One thickness-dependent factor does not appear on the curves. For the thinnest ($6\ \mu\text{m}$) cells the storage state is not as stable as for the thicker cells. The amount of attenuation of the direct beam varies with time after the cell is activated into the storage mode. This is a partial reversion to the clear state which reaches saturation after about 30 minutes. It indicates that in these thin cells the wall forces dominate over the volume forces.

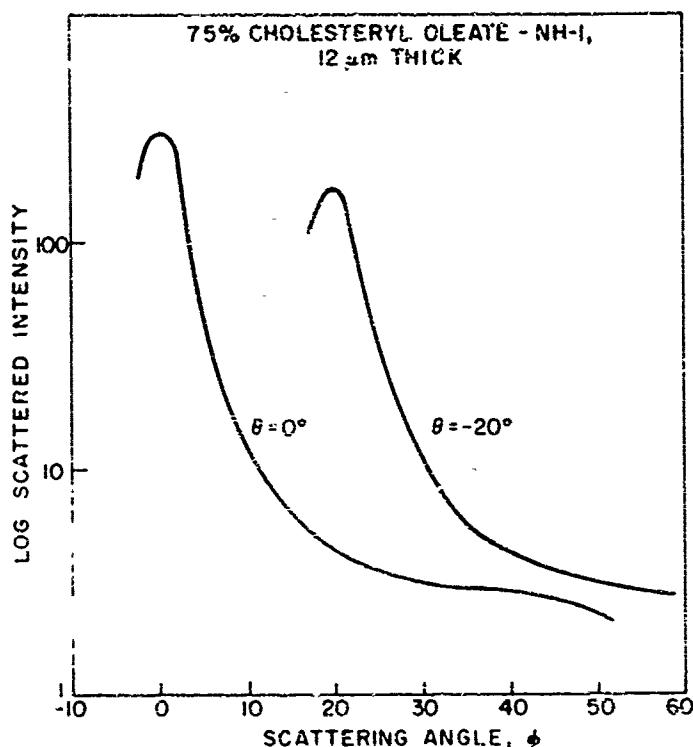


Figure 22. Angular light intensity as a function of incidence angle.

The measurements described up to now were all taken with the illuminating light beam perpendicular to the cells. This is not necessarily the geometrical arrangement in which these cells would be used for storage or display. We, therefore, performed scattering measurements where both the incoming direction and scattering direction were varied. The scattering for two different directions of ϕ (Figure 15) are compared in Figure 22. They show that the light scattering appears to depend mainly on $(\theta + \phi)$, i.e., on the relative scattering angle from input to output, rather than on the orientation of the cell (θ or ϕ separately). This is shown in more detail in Figure 23 where we plot the scattering intensity at fixed values of $(\theta + \phi)$.

To explain this behavior let us first consider the attenuated direct beam: $(\theta + \phi = 0)$. If the material is uniformly scattering, the attenuation is given by Eq. (2) with d replaced by the actual thickness traversed by the beam, namely $d/\cos \phi$. This quantity is shown by the dashed curve in Figure 23. The agreement with experiment is only qualitative. The same consideration would also apply if most of the scattering takes place in two layers next to the surfaces. At large scattering angles there is no drop of the scattered intensity at large angles of incidence. An explanation of this phenomenon will have to await a more detailed knowledge of the microscopic structure of the texture.

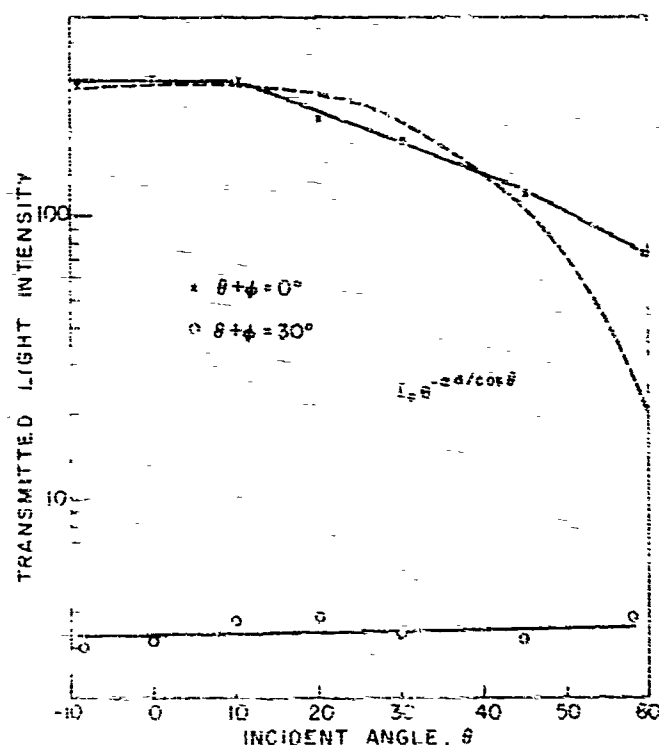


Figure 23. Variation of scattered light intensity with angle of incidence.

B. DISCUSSION OF RESULTS

A number of features emerge from the scattering measurements which have application to the design of cells for optimum display characteristics. Most importantly, the scattering of the storage state does not depend much either on the proportion of cholesteric material in the mixture or on the cell thickness. Since both of these variables have important influence on other properties of the cells, particularly the response speed, one will be able to select the parameter values to optimize these other properties.

The contrast ratio, for a given material, is mainly determined by the scattering of the clear state. What controls this variable property is not clear, but it appears to be related to surface effects. Further investigation of methods to treat the surface is required.

One of the major material parameters that influence the scattering of the storage state is the pitch of the cholesteric helix. We have seen that the Bragg scattering produces a large fraction of the light intensity at typical viewing angles. Values up to 40 or 50 deg will generally be required for viewing in transmitted light so that the value of the helical pitch should be about $1.5 \mu\text{m}$.

SECTION V MECHANISMS AND FUNDAMENTALS

Just as in nematic material, cholesteric material may be composed of molecules which have, individually, a dielectric anisotropy. If the anisotropy is positive, i.e., with the dipole pointing in the direction of the molecule, a strong electric field will have enough electrostatic energy to "unwind" the cholesteric helix to form a quasi-nematic texture. This is an optically clear state. When the field is removed, the cholesteric helices reform, resulting in a light scattering (focal-conic) texture. With materials of negative dielectric anisotropy, i.e., with dipoles perpendicular to the molecular axis, an external field will result in those dipoles turning parallel to the field. If the material is originally in the planar texture, the field can have no effect other than improving that texture, i.e., making it more perfect. If, however, the material is in a disrupted state, e.g., the scattering or focal-conic state, the field will act to convert it to the planar texture. This is the mechanism for "erasure" of the storage state. The "write" mechanism relies on the fact that when the frequency is low enough, the transit of ions can disrupt the planar texture, converting it to a focal-conic texture (much in the same way as dynamic scattering affects the nematic state). These results are summarized in Figure 24.

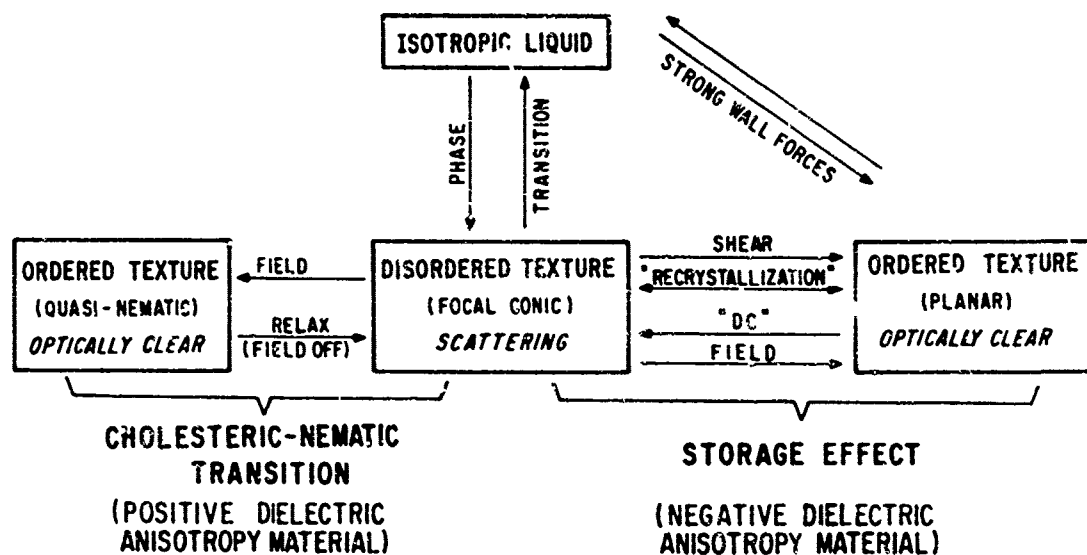


Figure 24. Schematic representation of electrically induced texture changes.

There is at each frequency (and dc), but below a critical frequency, a voltage at which an undisturbed planar texture is converted to the stored texture. This can be considered a threshold voltage; below this voltage, there is no disturbance of the planar texture and therefore no storage. To erase, a voltage must be applied of sufficiently high frequency to have no ionic effects. The field can then act on the negative dielectric anisotropy of the material to convert it to the planar (clear) texture. This frequency has been measured in the mixture of NH-1 and 7.5% cholesteryl oleate as a function of temperature (and thus of σ , the conductivity). At 45 V rms, the frequency at which the material changed from storage to clear (f_c) varied from 52 Hz at 25°C to 1250 Hz at 82°C. This variation was proportional to σ as found by plotting σ vs. f_c with temperature as a parameter. Such behavior is similar to the reported [19] variation of the threshold for dynamic scattering.

Above the threshold, a voltage can be used to write or erase by a small frequency shift, centered around f_c .

The fact that the planar texture can be induced with an applied field has been used to improve the off state in the storage-effect samples by applying the field to the cells while they were isotropic, then cooling. This resulted in a clearer off state and thus a better contrast ratio. The texture was so "good" that when the erase field was removed, no optical change was noticed in the cell. After storing for a time, the erased state was restored and was equally "good". Note that the storage material system is the only system that can be improved by the application of a high field during cell fabrication and which will result in a better contrast ratio.

One of the most important parameters to consider in any discussion of the mechanism of this effect is the pitch of the helix in these cholesteric materials. Efforts to measure this pitch for a variety of materials are currently under way. We have purchased a Zeiss circle polarimeter (0.01°) and expect to measure the optical rotary power of these materials in both the isotropic and anisotropic states to determine the relationship (if one exists) between the chirality of the helix and the chirality of the molecule.

The first approach involves a study of the effect of temperature on optical rotary power, and a special cell for use in the Zeiss polarimeter was designed and built. Measurements of the magnitude and sign of the optical rotation for a variety of compounds and mixtures were initiated only recently. Unfortunately, no significant conclusions could be drawn from these very limited data.

SECTION VI STATE-OF-THE-ART DEVICES

Earlier in this contract year (June 1971) a preliminary design plan was presented for a storage display panel which attempted to simulate the operation of a *glide-path indicator*. The relative merits of such a display application were reviewed* in consideration of the already existing electronic techniques utilized in military aircraft during controlled instrument landings. The relative simplicity of these existing ILS procedures and the conditioned pilot's experience with familiar instrument presentations are strong arguments against a new type of glide-path display system with storage capability. A further discouragement of the proposed liquid crystal glide-path indicator is the necessity to introduce an analog-digital converter to interface the available electronic information (in analog form) from the aircraft receiving systems with the X-Y addressed liquid crystal display.

In view of these restrictions and disadvantages, an alternate type of storage display panel has been devised. Though fundamentally similar to the glide-path indicator, this display presents the pilot (or navigator) with a ground location marker determined by the intersection of two radial beams transmitted from omnidirectional navigation stations.

The display panel is shown in Figure 25: it consists of two flat glass plates with a number of transparent electrode stripes present on each plate. However, unlike the usual linear X-Y format (columns and rows), the electrode stripes on each plate are extended in a radial fashion to accurately represent the radiation pattern transmitted in any 180° arc by the omnidirectional ground station. In actual practice it would be necessary to fabricate two separate devices, each presenting directional information received from only one transmitting navigation station. This would allow the system to be used with any two navigation stations regardless of their relative geographic positions. In addition, a moving map overlay would be required to locate specific areas over which the aircraft was scheduled to fly. A top view of one of these devices showing the electrode pattern is given in Figure 26.

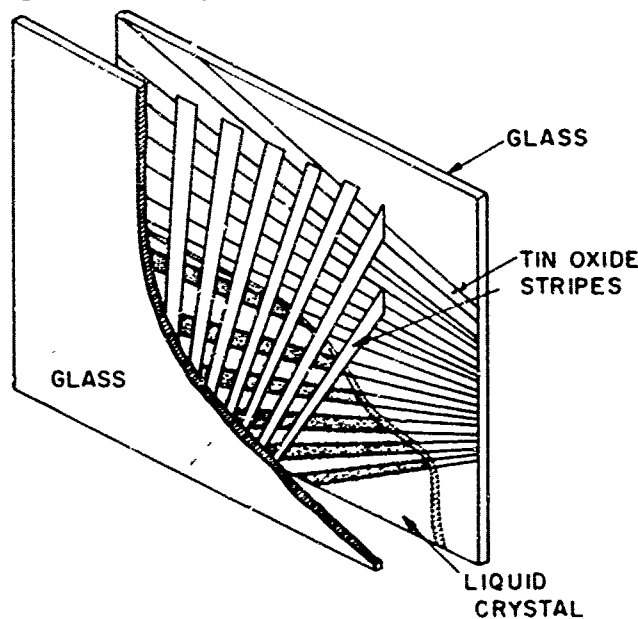


Figure 25. Liquid crystal panel for ground position locator.

*We wish to thank members of the AF Materials Laboratory and the Flight Dynamic Laboratory for their active participation in an informative open discussion of military ILS techniques during our visit in July.

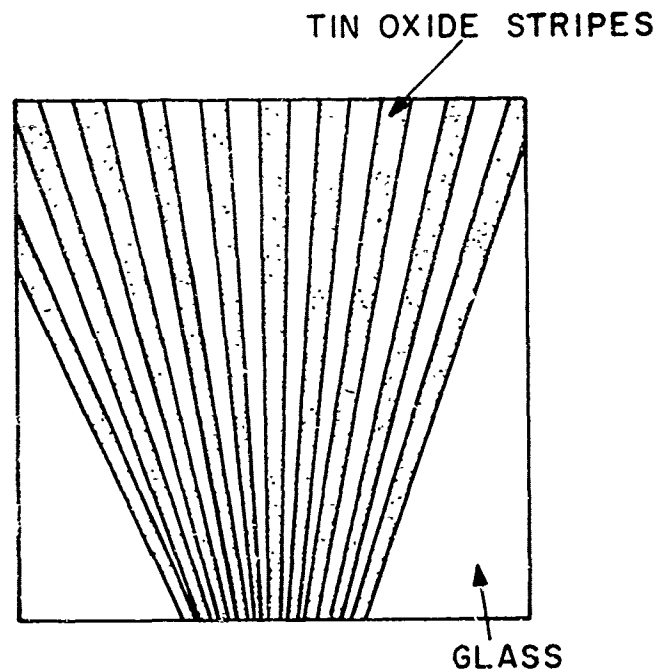


Figure 26 Top view of storage cell with patterned transparent conducting stripes.

Due to space limitations and wiring requirements, the display has nine "range legs" on each glass plate allowing a total of 81 discrete location markers on a 3.5-in. x 3.5-in. area of a standard aeronautical navigation map. The display presented on the prototype ground position locator was chosen so that the two transmitting navigation stations are conveniently located within the viewing area. For maximum contrast of the liquid crystal location marker it was necessary to displace the incident light beam from the transmitted light by some 35 to 45 degrees. An example of how this was accomplished is shown in Figure 27.

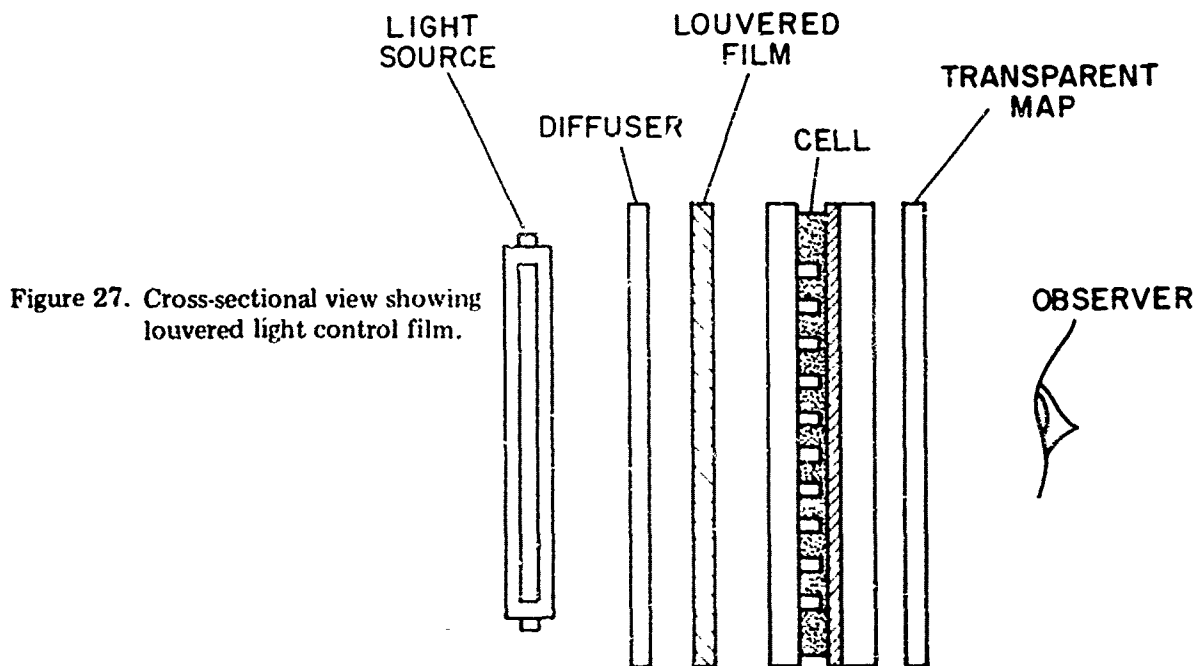


Figure 27. Cross-sectional view showing louvered light control film.

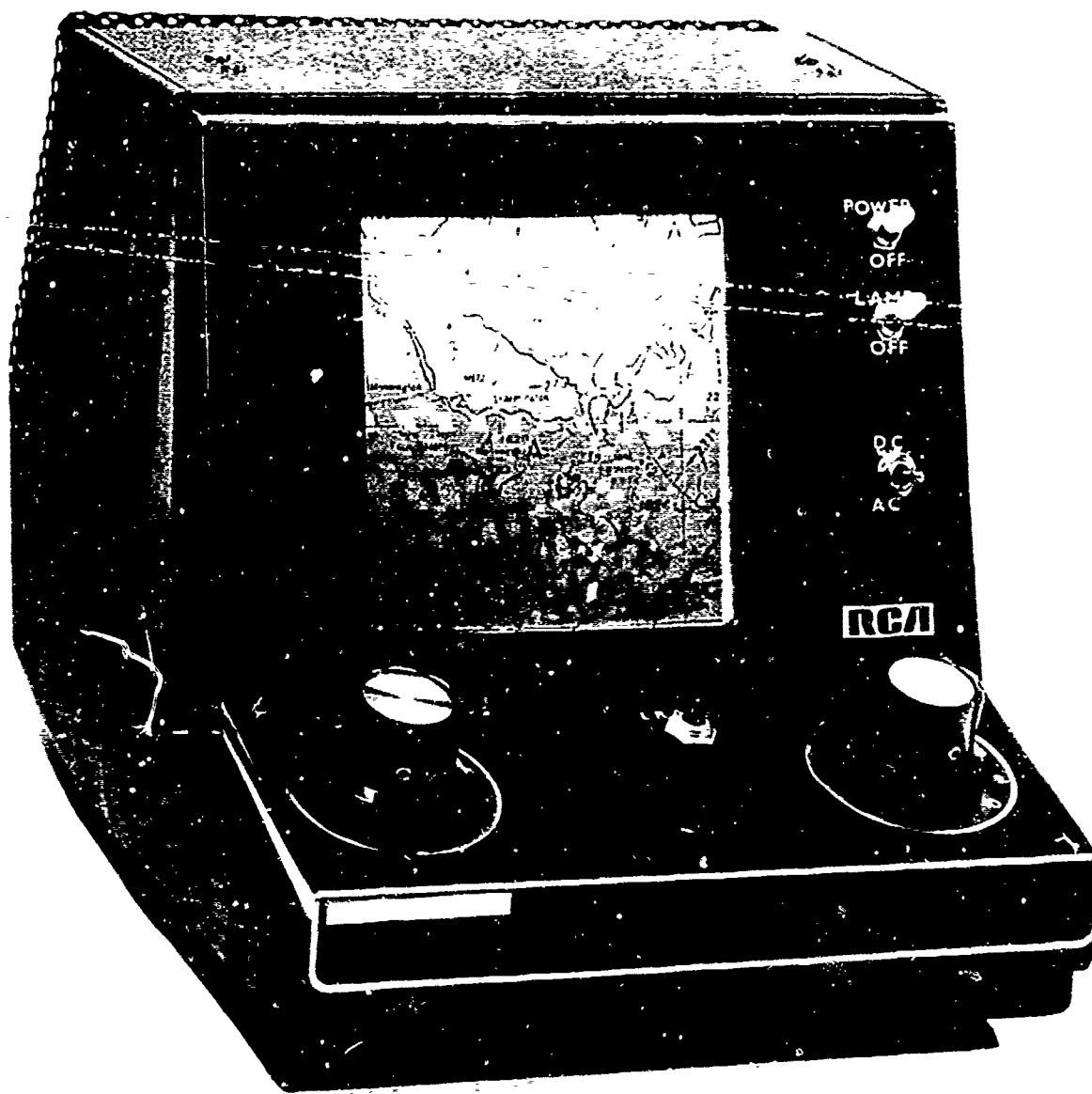


Figure 29. Simulated airborne ground position locator.

A simplified description of the method of operation requires only one stripe on each opposing glass surface to be electronically addressed. The directional information supplied to each plate selects a particular stripe corresponding to a radial direction from adjacent navigation stations. One omnidirectional station selects an appropriate stripe on the top glass, the second station determines a corresponding stripe on the bottom plate. By choosing an appropriate dc bias or "write" voltage to activate the selected lines, an opaque area appears only at the intersection of the addressed stripes. This opaque area is highly light scattering off-axis from the incident light beam and provides a discrete illuminated area to be positively located on the transparent navigational chart (see Figure 27). Increasing the magnitude of the "write" signal allows the entire segmented length of the two activated radial lines to be clearly visible. The pictorial information such a display might present is shown in the photograph of Figure 25. In this simulated display, the extended radial lines represent the directional path to (from) the chosen navigation stations and the intersection of these two lines corresponds to the aircraft's relative ground location.

Since no power is required to maintain the activated areas in their scattering state (storage mode), the panel is ready to receive and display similar information at any later time, thus maintaining a ground track history of the aircraft's flight path. Erasure of unwanted "stored" information is accomplished by merely replacing the dc "write" voltage with an appropriate high-frequency signal. A schematic diagram of the electronic control circuit for this simulated display is shown in Figure 29.

It should be understood in the operation of a practical device that the navigational stations need only to provide the necessary directional information to *select* the desired radial lines on the liquid crystal cell. The actual "write" and "erase" signals applied to the liquid crystal material between these selected lines can easily be obtained from an internal low power supply.

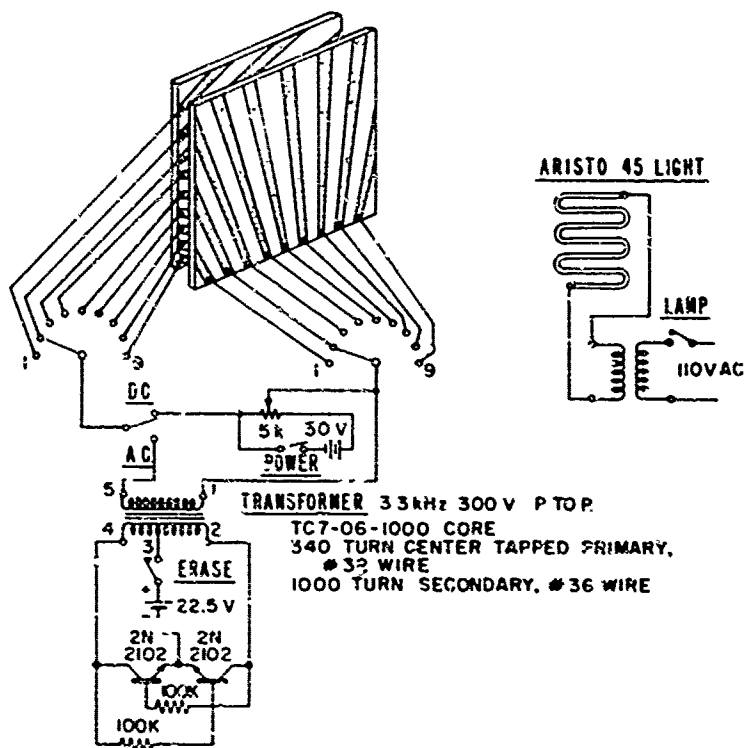


Figure 29. Schematic diagram of simulated ground position locator.

SECTION VII

CONCLUSIONS AND RECOMMENDATIONS

The materials research effort has been divided into two parts. In the first part a search for broad-range nematic materials with negative dielectric anisotropy led to the synthesis of a homologous series of p-alkoxybenzylidene-p-aminophenyl acrylates and p-alkoxybenzylidene-p-aminophenyl n-alkyl carbonates. Mixtures of selected compounds from the former series were prepared and one "room-temperature" ternary mixture (NH-1), which exhibited nematic behavior from 25 to 105°C, was found. A ternary mixture (NH-2) prepared with compounds from the latter series had a nematic range of 30 to 118°C but it exhibited poorer dynamic scattering characteristics than NH-1.

The second part of the materials program was concerned with the preparation of Schiff base derivatives which exhibited cholesteric mesomorphism. A group of optically active benzylidene aniline derivatives having alkoxy and acyloxy groups with asymmetric carbon atoms were prepared, and the compounds were found to exhibit cholesteric mesomorphism. One of these compounds, *l*-p-anisylidene-p-aminophenyl 3-methylvalerate, had a cholesteric range of 41 to 78°C. Other derivatives which had asymmetric carbon atoms in the alkoxy portion of the molecules exhibited both smectic and cholesteric behavior. However, it was possible to prepare mixtures of these compounds with NH-1 to eliminate smectic mesomorphism.

The criterion by which the cholesteric-nematic systems under investigation were evaluated was their ability to modify incident light (reflection, transmission, contrast ratio) at moderate excitation voltages and to retain their scattering texture over a reasonable period of time with no maintaining power. Except for the materials containing less than 2% or greater than 20% cholesteric component, all of the mixtures satisfied these requirements to some degree. Electro-optic behavior of materials containing less than 2% cholesteric component was similar to that of dynamic scattering w. devices made with materials having greater than 20% cholesteric component exhibited cholesteric type characteristics. Test cells made with the cholesteryl oleate-NH-1 nematic mixtures - specifically in the 5 to 10% composition range - appear to be qualitatively superior in terms of display-related parameters. A particularly useful mixture contained 7.5% cholesteryl oleate and had a cholesteric range of 25 to 96°C. We recommend that more extensive measurements be made with the nonsteroidal cholesterics and, in particular, with mixtures containing both the steroidal and nonsteroidal cholesterics.

Standard test cells fabricated with 5 to 10% cholesteryl oleate-NH-1 mixtures exhibited writing speeds of 5 to 10 msec and erasure speeds of 0.5 to 1.0 sec at room temperature, using an appropriate ac drive signal of approximately 100 V (rms). With no excitation field applied, the contrast ratios were usually greater than 5:1, with maximum contrast occurring at the Bragg scattering angle displaced some 40 to 55° from the incident light. Storage properties appear to be one of the lesser problem areas. Unencapsulated cells stored in room ambient conditions have exceeded three months life testing with no objectional reduction in visual appearance or operating characteristics.

In order to establish the relationship between electro-optic behavior and molecular structure, capacitance and light-scattering measurements were made on selected cholesteric materials. The capacitance measurements enabled us to calculate a dielectric constant of 4.9 for the focal-conic (scattering) texture and 5.8 for the planar texture of 7.5% cholesteryl oleate in NH-1. This 20% variation in dielectric anisotropy is typical of the changes observed in pure nematic compounds. Light-scattering measurements led to a value of 1.6 μm for the helical pitch of 10% cholesteryl oleate in the standard nematic. We recommend that light-scattering measurements of this type be extended to other steroidal and nonsteroidal compounds in an effort to develop a better understanding of the relationship between helical pitch and molecular structure.

Rapid temperature changes partially converted the focal-conic texture of the material in the stored state to the clear planar texture. At constant temperature within the liquid crystalline range of the material, cells could be operated normally in both the storage and erase modes. In fact, some improvements in electro-optic properties were noted up to temperatures of 65°C.

Current experimental studies have suggested the probability of a specific materials resistivity range for optimum device performance. It appears that materials having a bulk resistivity of less than 10^{10} ohm-cm exhibit response characteristics superior to devices made with higher resistivity materials. Further work on establishing optimum resistivity levels should be done.

On the basis of the experiments described above the mechanism of the optical storage phenomenon appears to involve a change from the "clear", planar texture of the cholesteric mesophase to the scattering, focal-conic texture by the turbulent motion of ions in transit through the ordered liquid. When the electric field is removed the turbulence ceased but the quasi-stable, focal-conic texture remains. The application of a high-frequency signal produces a reorientation of molecules and, hence, a reversion to the stable planar texture.

A state-of-the-art storage device was constructed which would serve as the display unit in an airborne ground location system. It would provide the pilot or navigator of an aircraft with a map presentation of the past and present position of his aircraft in relation to two separate ground navigation stations.

REFERENCES

1. G. Friedel, *Ann. Physique*, 18, 273 (1972).
2. F. J. Kahn, *Appl. Phys. Letters*, 18, 231 (1971).
3. R. Cano, *Bull. Soc. Fr. Mineral. Cristallogr.*, 90, 333 (1967); G. Durond, L. Leger, F. Rondelez, and M. Veyessie, *Phys. Rev. Letters*, 22, 227 (1969); and T. Nakagiri, H. Kodama, and K. K. Kobayashi, *Phys. Rev. Letters*, 27, 564 (1971).
4. G. W. Gray, *Molecular Structure and the Properties of Liquid Crystals*, (Academic Press, New York, 1962).
5. W. Helfrich, *J. Chem. Phys.*, 51, 4092 (1969).
6. K. Taniyama, T. Aoyagi, and S. Nomura, *Japan. J. Appl. Phys.*, 9, 584 (1970).
7. G. H. Heilmeyer and W. Helfrich, *Appl. Phys. Letters*, 6, 155 (1970).
8. G. H. Heilmeyer and J. E. Goldmacher, *Proc. IEEE*, 57, 34 (1969).
9. H. Kelker and B. Scheurle, *Angew. Chem. Intl. Ed.*, 1969, 884.
10. J. A. Castellano, M. T. McCaffrey, and R. Williams, results to be published.
11. J. A. Castellano, J. E. Goldmacher, L. A. Barton, and J. S. Kane, *J. Org. Chem.*, 33, 3501 (1968).
12. J. A. Castellano and J. E. Goldmacher, U. S. Patent 3,540,796.
13. G. W. Gray and B. Jones, *J. Chem. Soc.*, 1954, 1487.
14. A. I. Vogel, *Practical Organic Chemistry*, 3rd Ed., (John Wiley and Sons, Inc., New York, 1966) p. 253.
15. P. A. Levene and R. E. Marker, *J. Biol. Chem.*, 91, 77 (1931).
16. W. Haas, J. Adams, and B. J. Flannery, *Phys. Rev. Letters*, 24, 557 (1970).
17. Orsay Liquid Crystal Group, *Phys. Rev. Letters*, 25, 1642 (1970).
18. G. H. Heilmeyer, L. A. Barton, and L. A. Zanoni, *Proc. IEEE*, 56, 1162 (1968).
19. R. B. Meyer, *Appl. Phys. Letters*, 12, 281 (1968); F. J. Kahn, *Phys. Rev. Letters*, 24, 209 (1970).